

非传统稳定同位素地球化学： 历史与展望

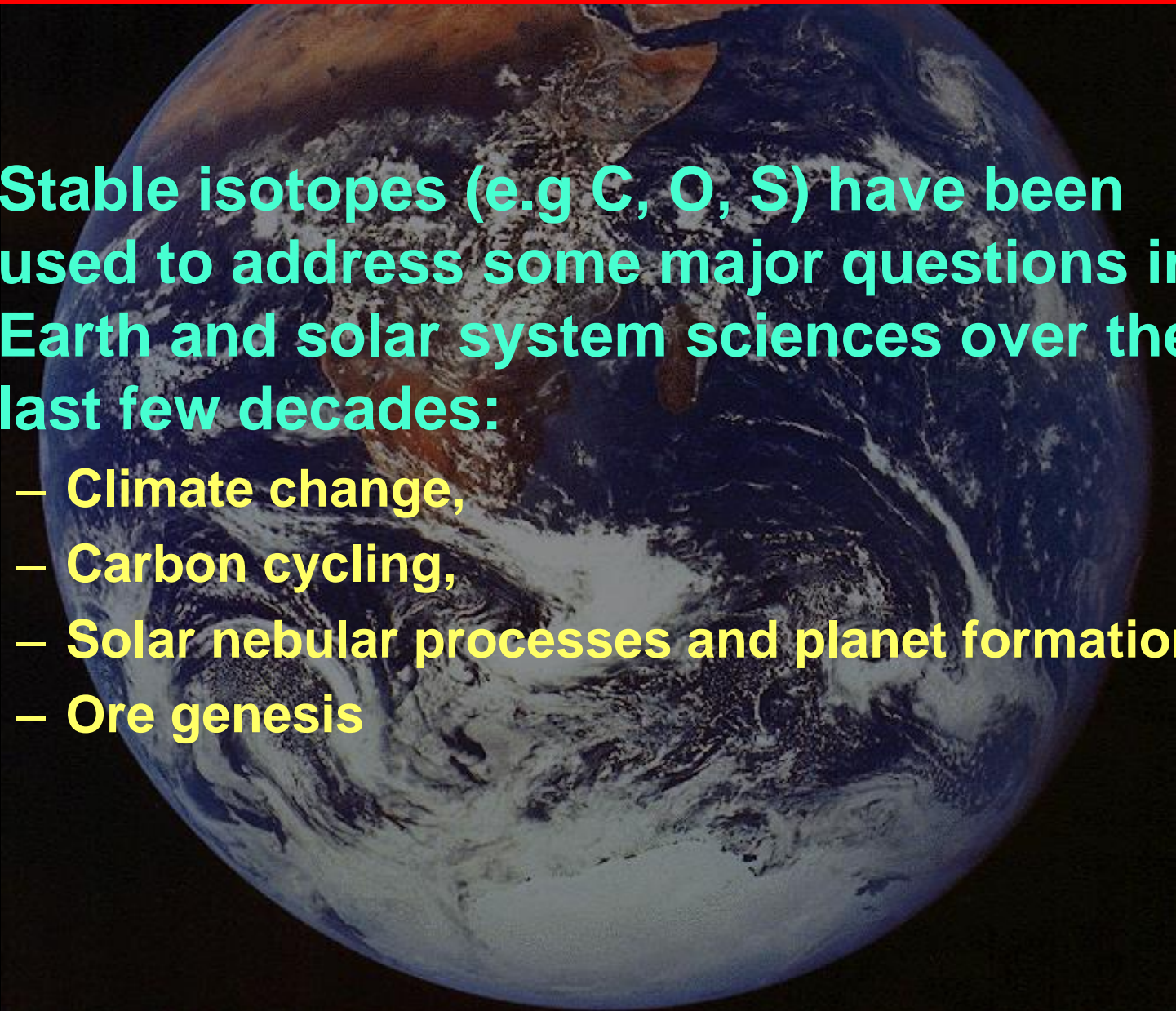
朱 祥 坤

中国地质科学院地质研究所

- **Non-traditional stable isotopes & why**

Traditional & Non-traditional Isotopes

- Stable isotopes (e.g C, O, S) have been used to address some major questions in Earth and solar system sciences over the last few decades:
 - Climate change,
 - Carbon cycling,
 - Solar nebular processes and planet formation,
 - Ore genesis



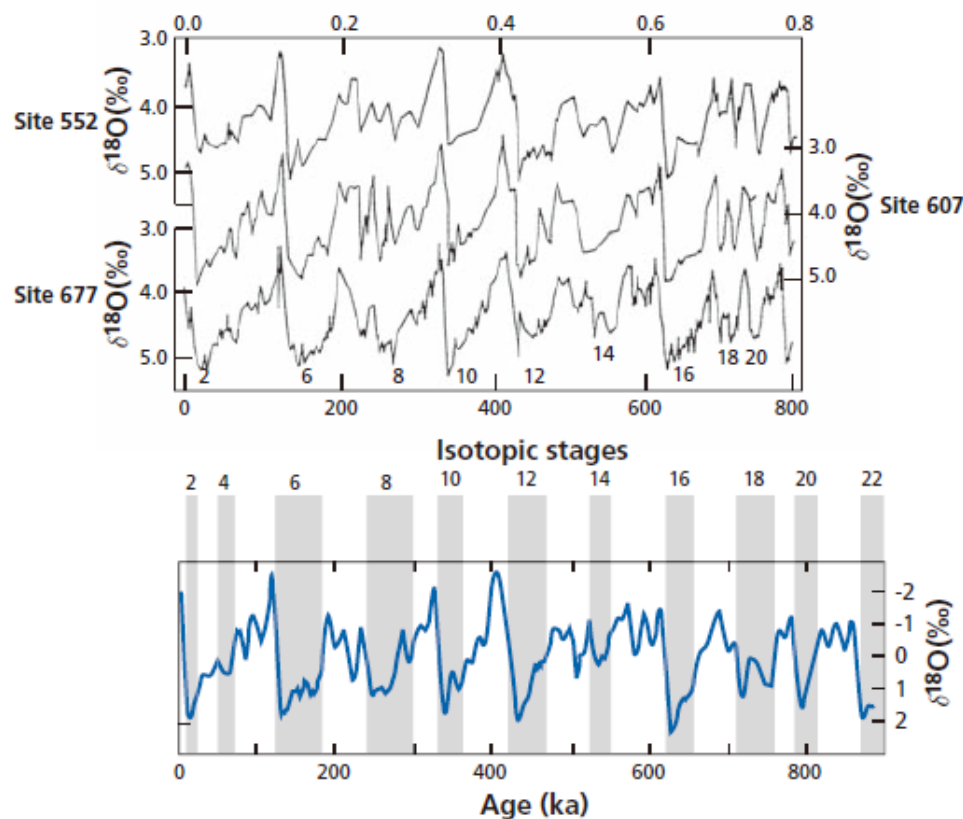


Figure 7.35 Records of $\delta^{18}\text{O}$ in foraminifera and the synthetic reference curve. (a) Record of $\delta^{18}\text{O}$ for benthic foraminifera at three sites: site 552 – 56° N, 23° W in the North Atlantic; site 607 – 41° N, 33° W in the mid Atlantic; site 667 – 1° N, 84° W in the equatorial Pacific. Correlation between the three cores is excellent. (b) Synthetic reference curve produced by tuning, which consists in defining the timescale so that the Fourier decomposition frequencies of the $\delta^{18}\text{O}$ values of the cores match the astronomical frequencies from Milankovitch's theory. The period is then subdivided into isotopic stages. The odd stages are warm periods and the even stages (shaded) glacial periods. (Notice that the interglacials correspond to increased $\delta^{18}\text{O}$ values and fluctuations are just a few per mill.) After various compilations from Bradley (1999).

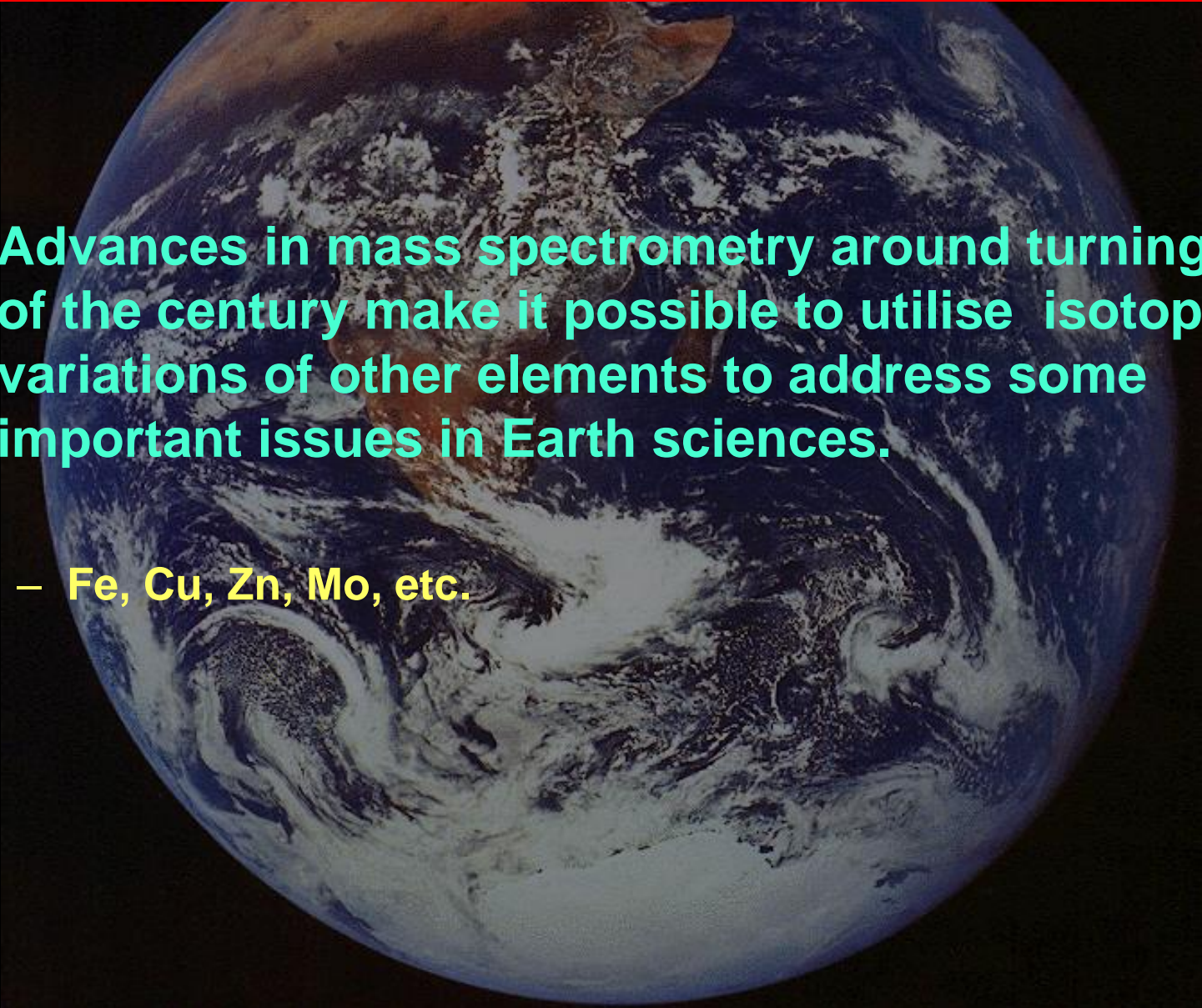


海洋原生动物——有孔虫
Marine Protozoa —— Foraminifera

单细胞动物

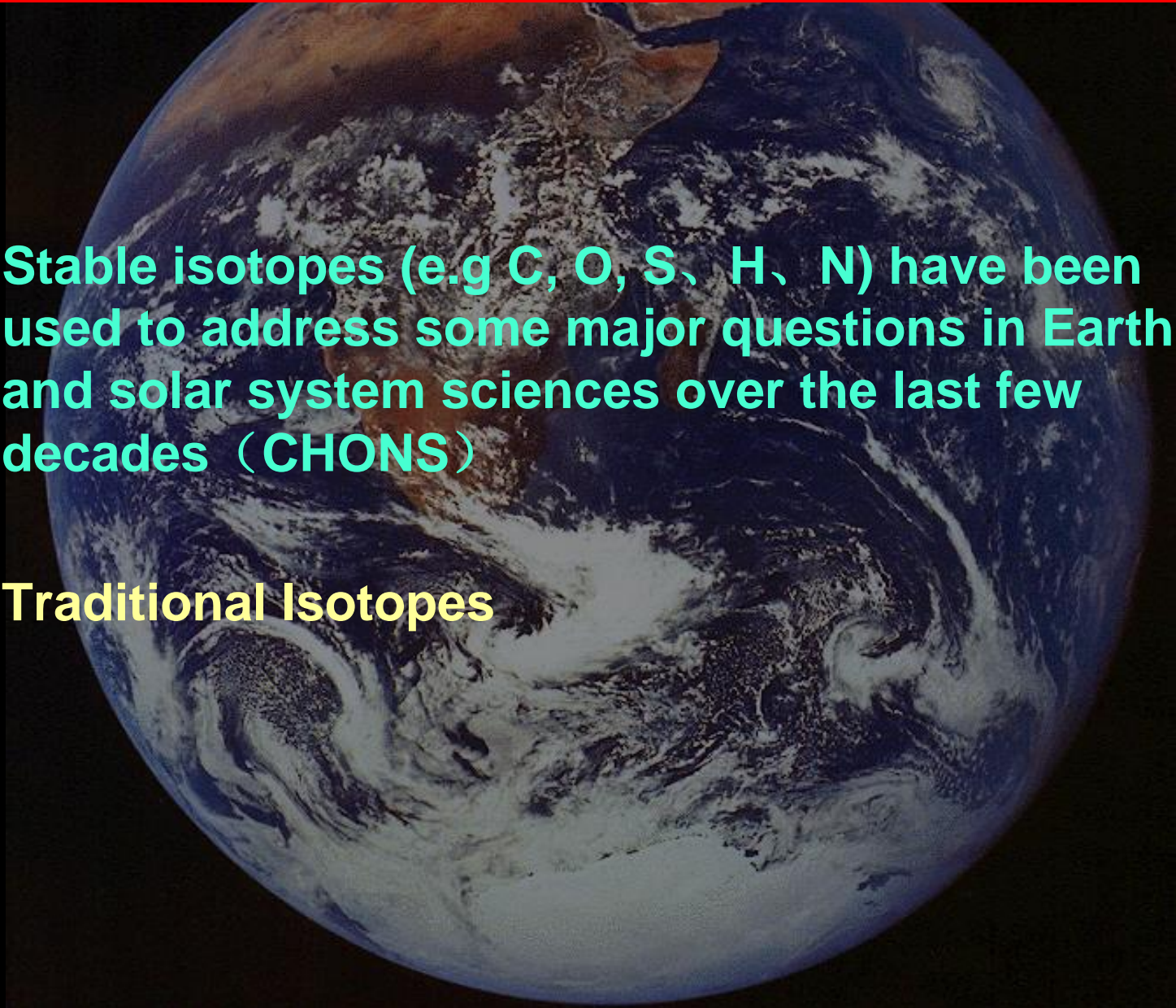
Traditional & Non-traditional Isotopes

- Advances in mass spectrometry around turning of the century make it possible to utilise isotope variations of other elements to address some important issues in Earth sciences.
 - Fe, Cu, Zn, Mo, etc.

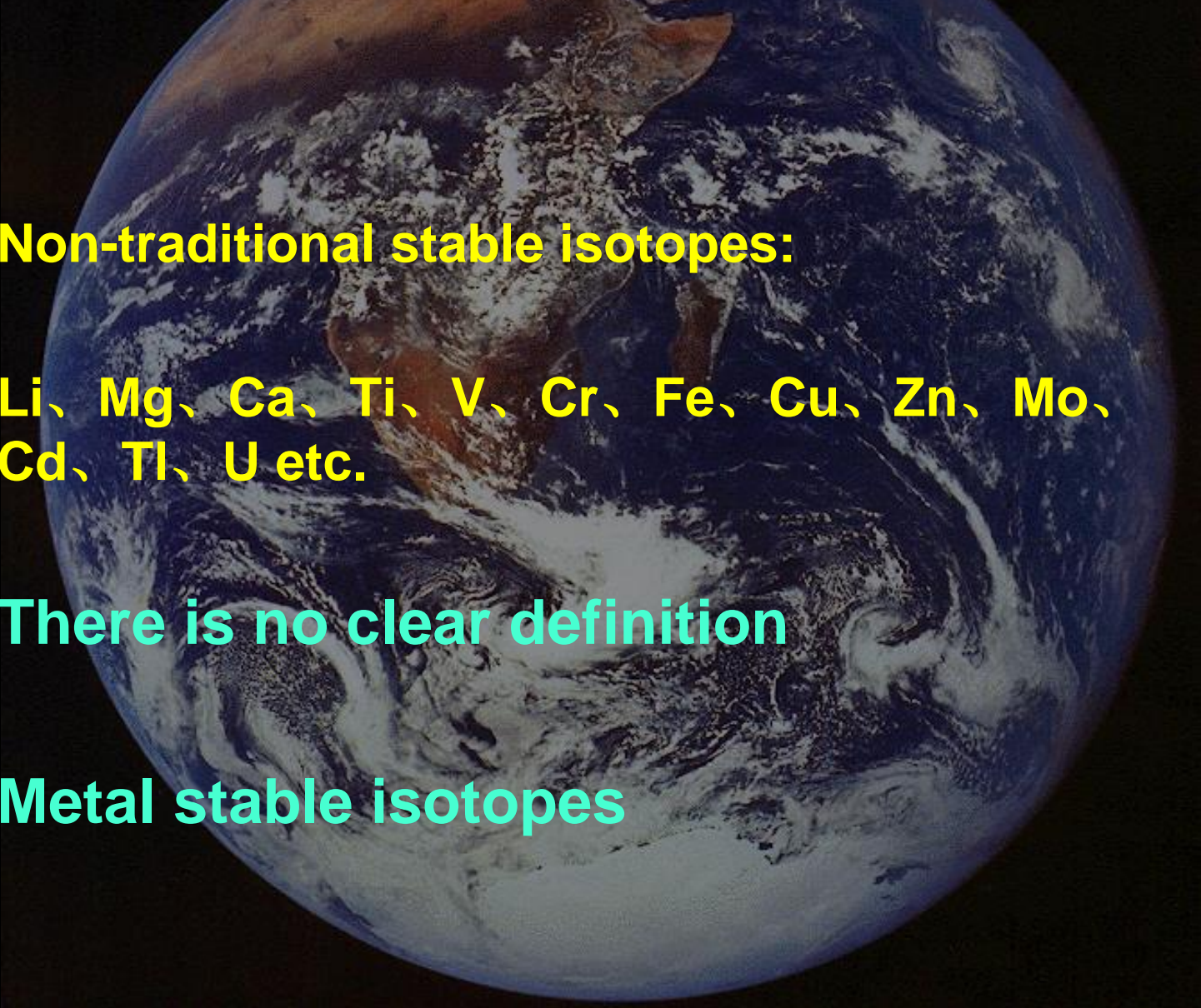


Traditional & Non-traditional Isotopes

- Stable isotopes (e.g C, O, S, H, N) have been used to address some major questions in Earth and solar system sciences over the last few decades (CHONS)
- Traditional Isotopes

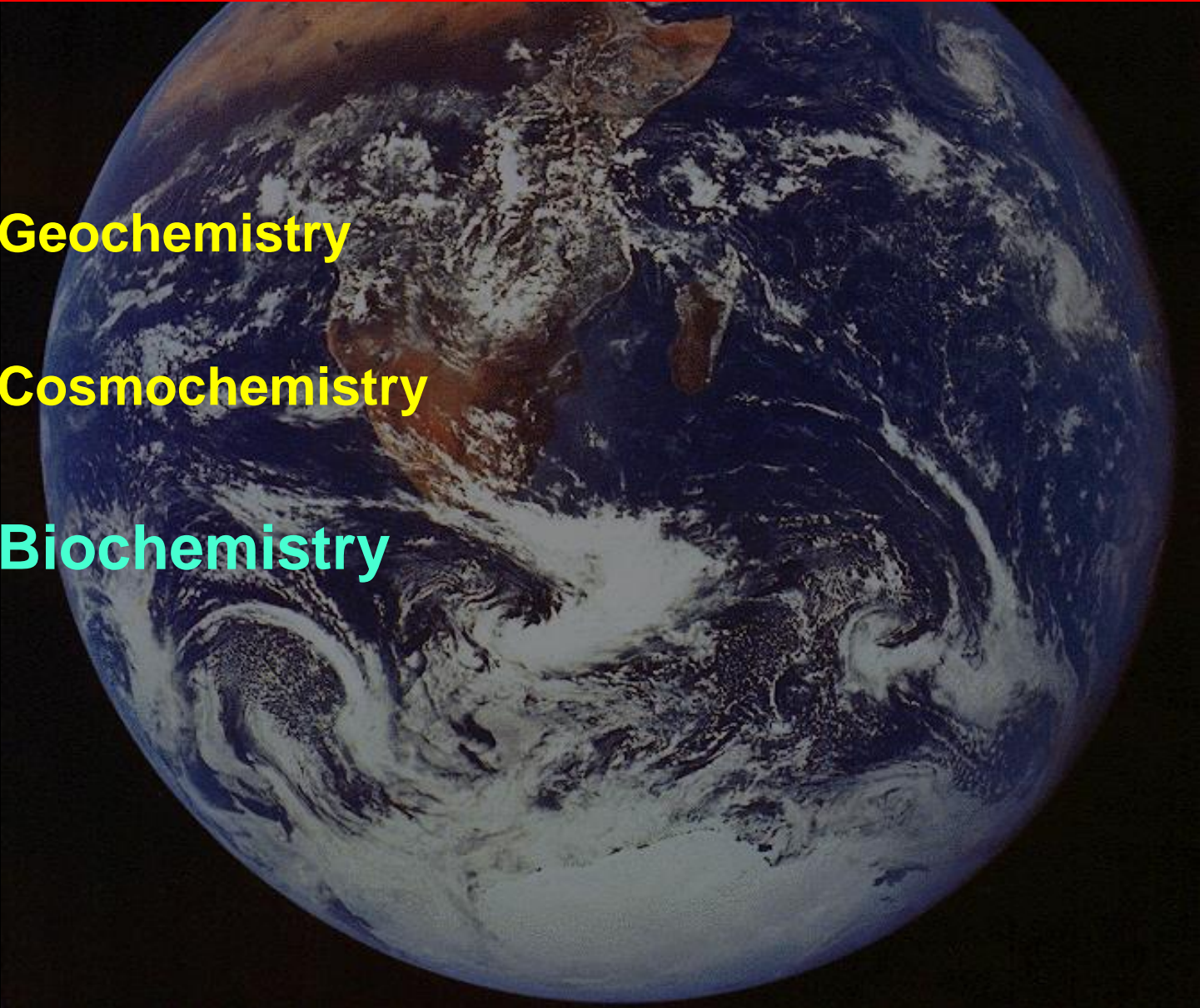


Traditional & Non-traditional Isotopes

- **Non-traditional stable isotopes:**
 - **Li, Mg, Ca, Ti, V, Cr, Fe, Cu, Zn, Mo, Cd, Tl, U etc.**
 - **There is no clear definition**
 - **Metal stable isotopes**
- 

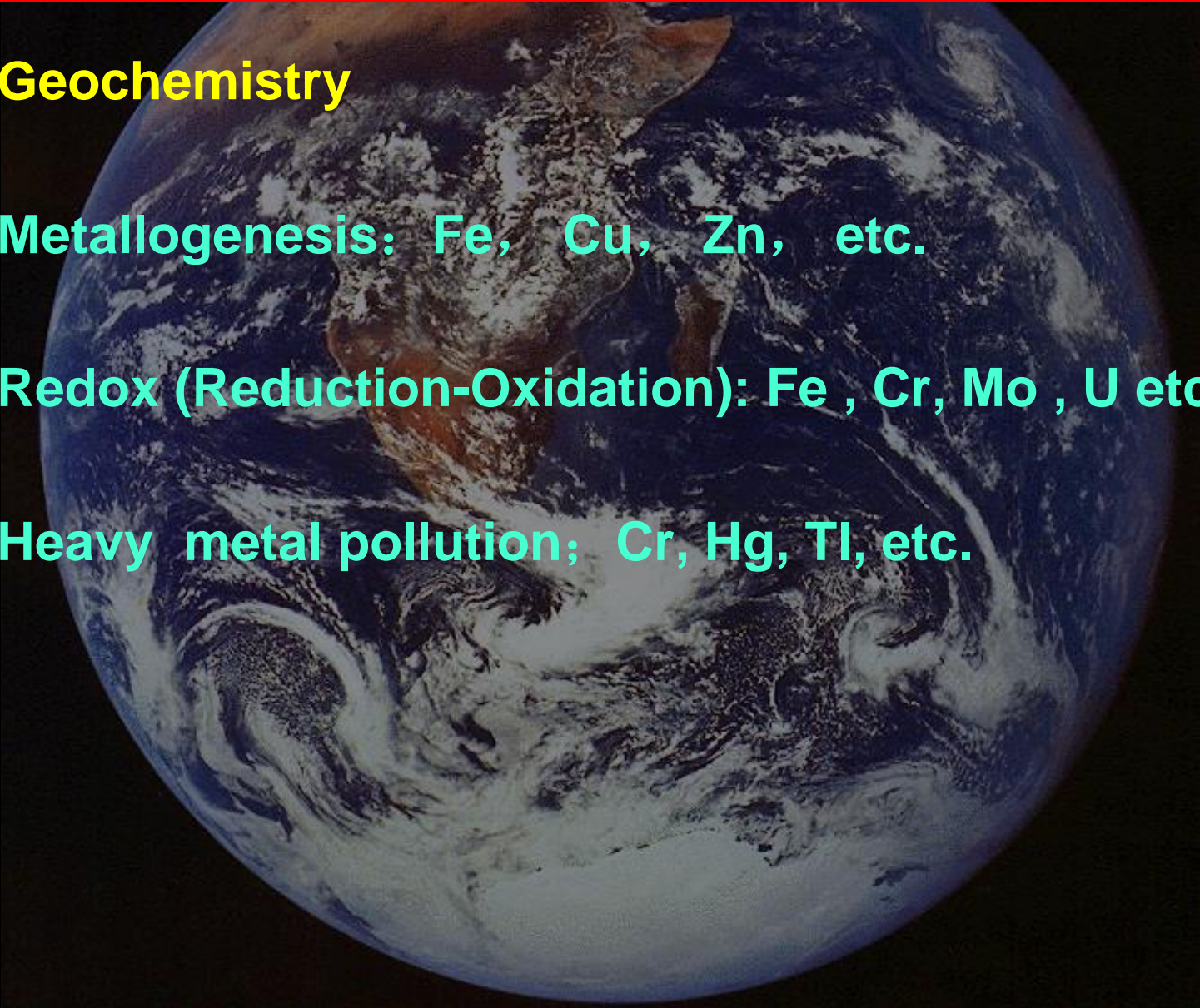
Why Non-traditional Isotopes?

- **Geochemistry**
- **Cosmochemistry**
- **Biochemistry**



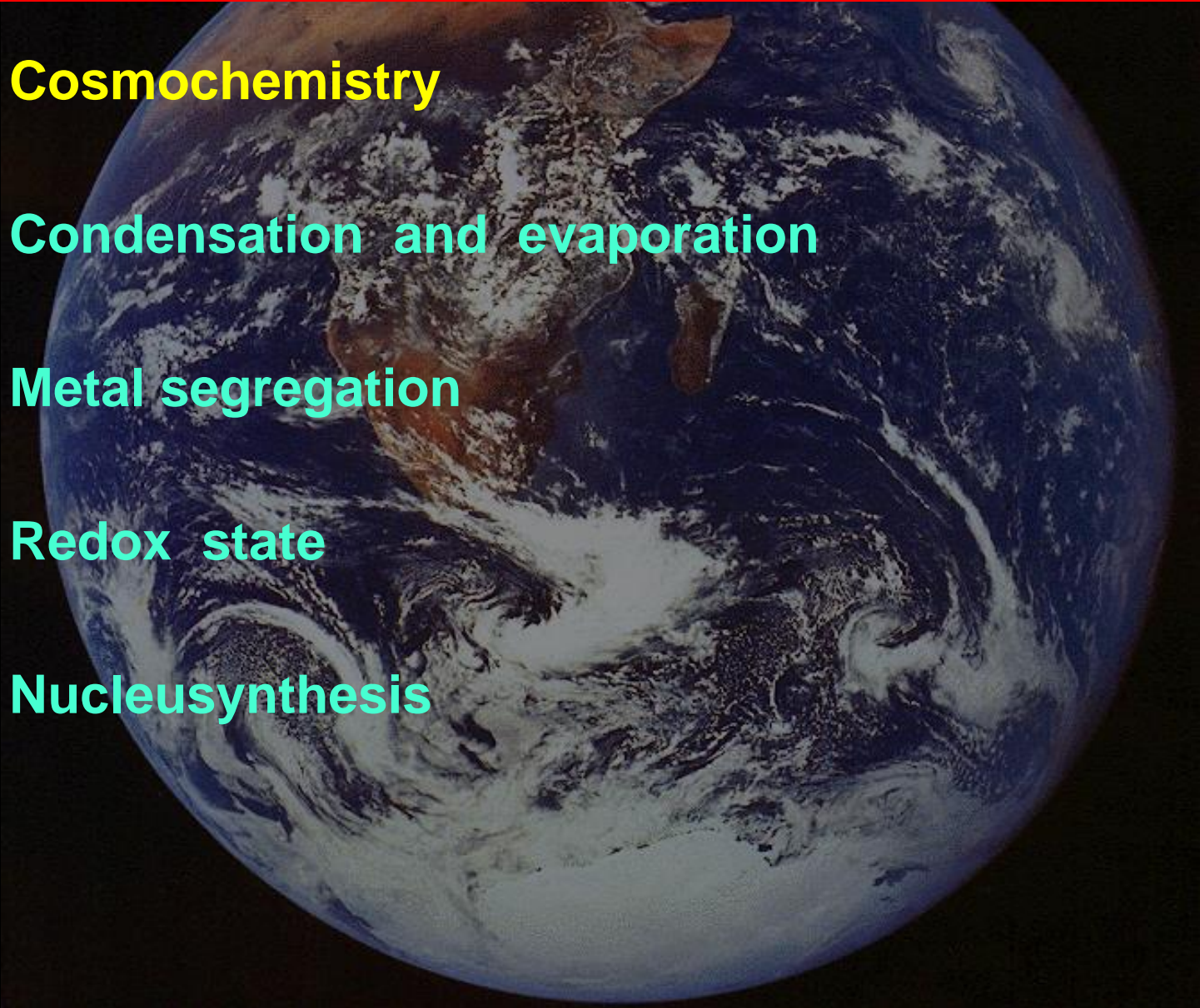
Why Non-traditional Isotopes?

- **Geochemistry**
- **Metallogenesis: Fe, Cu, Zn, etc.**
- **Redox (Reduction-Oxidation): Fe, Cr, Mo, U etc.**
- **Heavy metal pollution; Cr, Hg, Tl, etc.**



Why Non-traditional Isotopes?

- **Cosmochemistry**
- **Condensation and evaporation**
- **Metal segregation**
- **Redox state**
- **Nucleosynthesis**



天体物理学家玛格丽特·伯比奇辞世：她用这篇跨时代的论文，揭开宇宙元素起源的关键一环

环球科学 6天前

以下文章来源于原理，作者不二北斗



原理

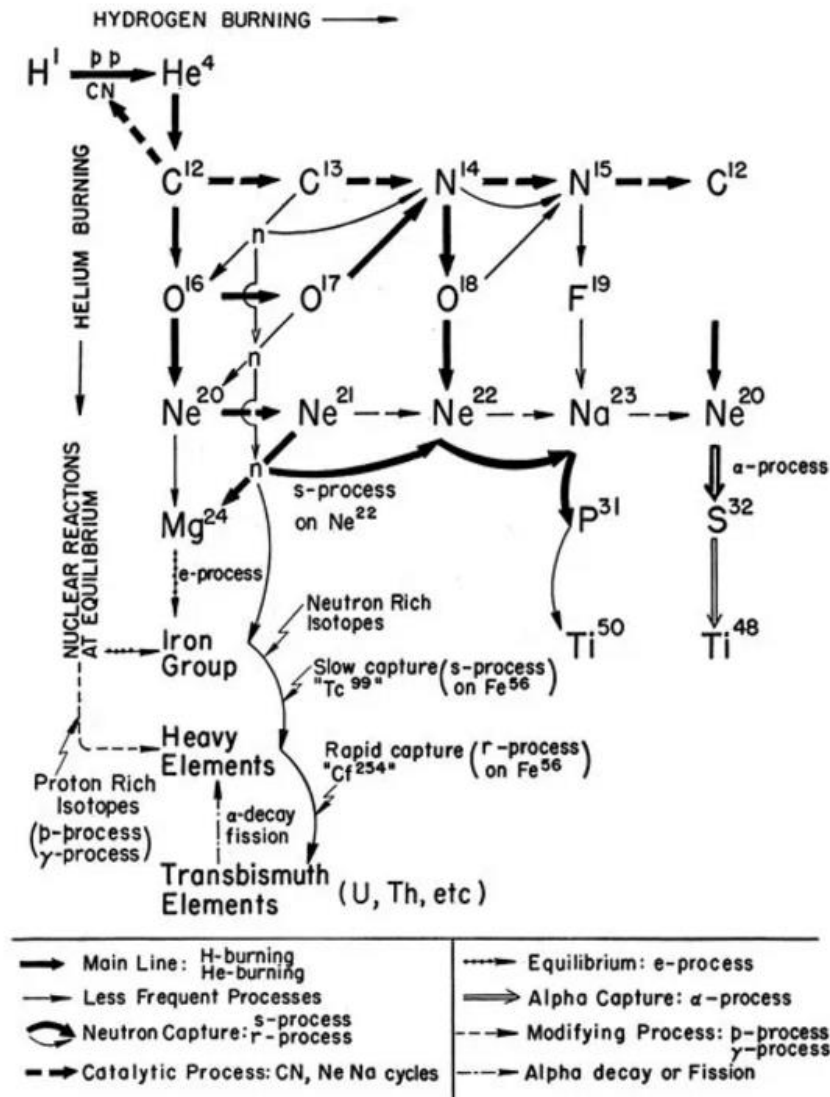
科学，照亮黑暗的蜡烛。



玛格丽特·伯比奇 (Margaret Burbidge, 1919 - 2020) | 图片来源: Annie Gracy/Wikipedia

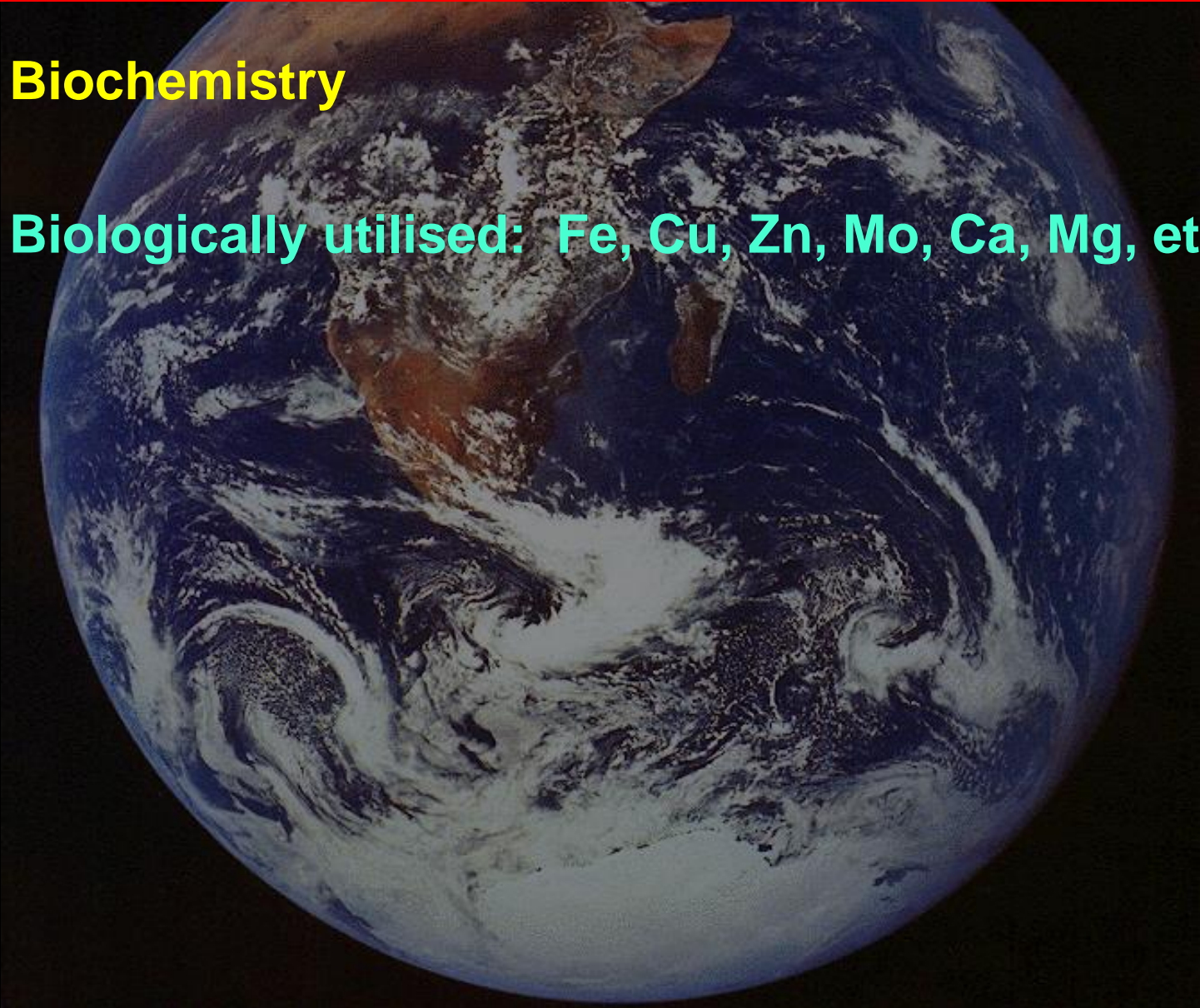
她是一位极具天赋的科学家，同大多数优秀的女性科学家一样，她也没有逃过时代背景给她带来的残酷挑战。在她的科学生涯中，曾多次遭遇因性别歧视带来的不公，但她仍然成为了天文学界最有影响力的天体物理学家之一，留下了不朽的科学瑰宝，她就是玛格丽特·伯比奇 (Margaret Burbidge)。

与她一同完成这一伟大成就的科学家还有她的先生杰弗里·伯比奇 (Geoffrey Burbidge)、威廉·福勒 (William Fowler) 和弗雷德·霍伊尔 (Fred Hoyle)。这篇奠基性的论文的标题为《恒星中的元素合成》，人们常以这四位作者的姓氏开头字母将其简称为**B²FH**。这篇论文是目前天文学家**理解恒星核合成 (恒星将氢和氦等元素锻造成宇宙中更重的元素)**的基础，为化学元素的宇宙起源奠定了基础。



Why Non-traditional Isotopes?

- **Biochemistry**
- **Biologically utilised: Fe, Cu, Zn, Mo, Ca, Mg, etc.**



Elements & Isotopes

1 H 1.008 Hydrogen																	2 He 4.0026 Helium				
3 Li 6.941 Lithium	4 Be 9.0122 Beryllium															5 B 10.811 Boron	6 C 12.011 Carbon	7 N 14.007 Nitrogen	8 O 15.999 Oxygen	9 F 18.998 Fluorine	10 Ne 20.189 Neon
11 Na 22.990 Sodium	12 Mg 24.305 Magnesium															13 Al 26.982 Aluminum	14 Si 28.086 Silicon	15 P 30.974 Phosphorus	16 S 32.065 Sulfur	17 Cl 35.453 Chlorine	18 Ar 39.948 Argon
19 K 39.098 Potassium	20 Ca 40.078 Calcium	21 Sc 44.956 Scandium	22 Ti 47.867 Titanium	23 V 50.942 Vanadium	24 Cr 51.996 Chromium	25 Mn 54.938 Manganese	26 Fe 55.845 Iron	27 Co 58.933 Cobalt	28 Ni 58.693 Nickel	29 Cu 63.546 Copper	30 Zn 65.38 Zinc	31 Ga 69.723 Gallium	32 Ge 72.630 Germanium	33 As 74.922 Arsenic	34 Se 78.96 Selenium	35 Br 79.904 Bromine	36 Kr 83.80 Krypton				
37 Rb 85.468 Rubidium	38 Sr 87.62 Strontium	39 Y 88.906 Yttrium	40 Zr 91.224 Zirconium	41 Nb 92.906 Niobium	42 Mo 95.94 Molybdenum	43 Tc 98 Technetium	44 Ru 101.07 Ruthenium	45 Rh 102.91 Rhodium	46 Pd 106.42 Palladium	47 Ag 107.87 Silver	48 Cd 112.41 Cadmium	49 In 114.82 Indium	50 Sn 118.71 Tin	51 Sb 121.76 Antimony	52 Te 127.60 Tellurium	53 I 126.905 Iodine	54 Xe 131.29 Xenon				
55 Cs 132.91 Cesium	56 Ba 137.33 Barium	57 - 71 La - Lu	72 Hf 178.49 Hafnium	73 Ta 180.95 Tantalum	74 W 183.84 Tungsten	75 Re 186.21 Rhenium	76 Os 190.23 Osmium	77 Ir 192.22 Iridium	78 Pt 195.08 Platinum	79 Au 196.97 Gold	80 Hg 200.59 Mercury	81 Tl 204.38 Thallium	82 Pb 207.2 Lead	83 Bi 208.98 Bismuth	84 Po 209 Polonium	85 At 210 Astatine	86 Rn 222 Radon				
87 Fr 223 Francium	88 Ra 226 Radium	89 Ac	90 Th 232.04 Thorium	91 Pa 231.04 Protactinium	92 U 238.03 Uranium																



Bulk biological elements



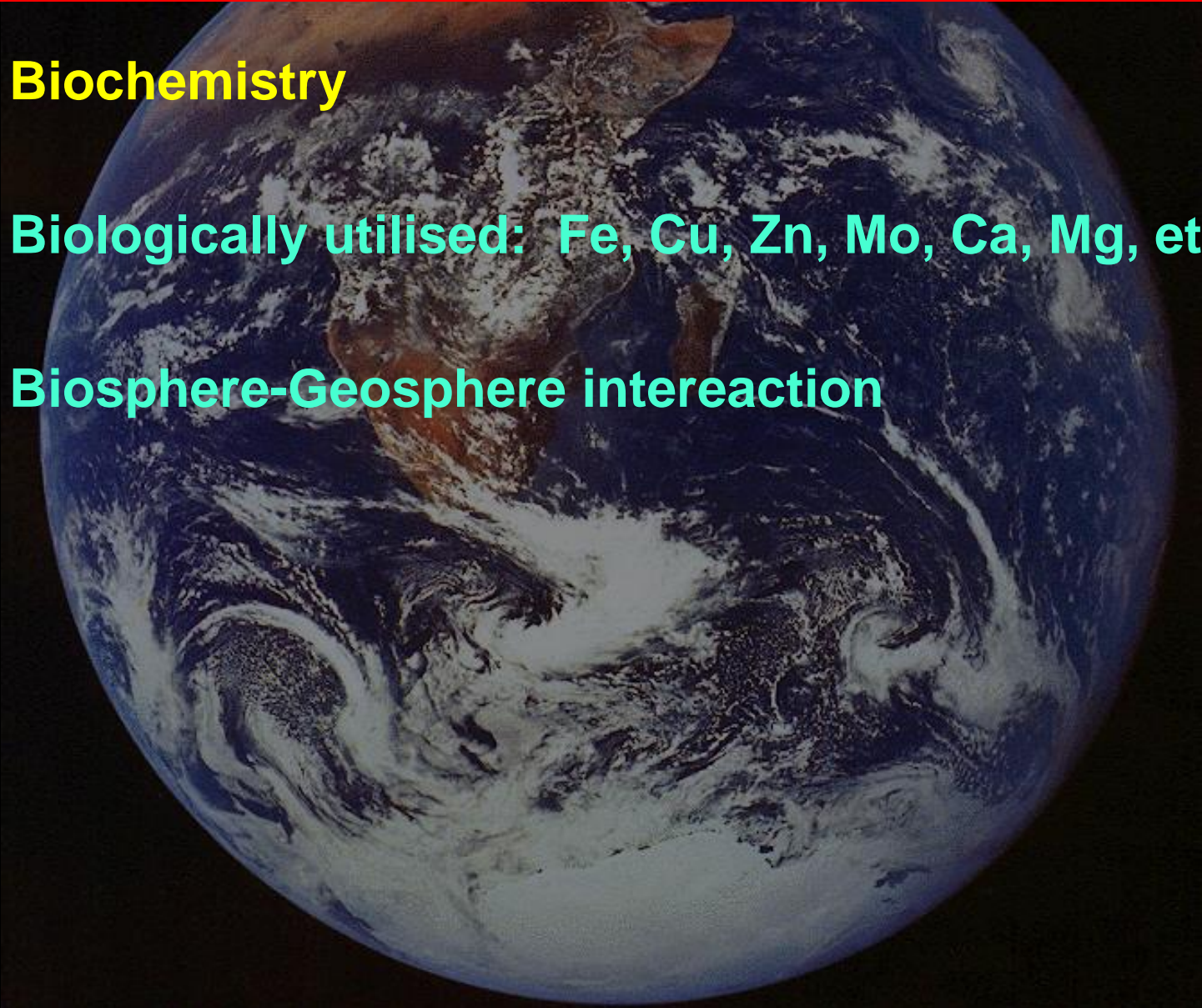
Trace elements believed to be essential for bacteria, plants or animals



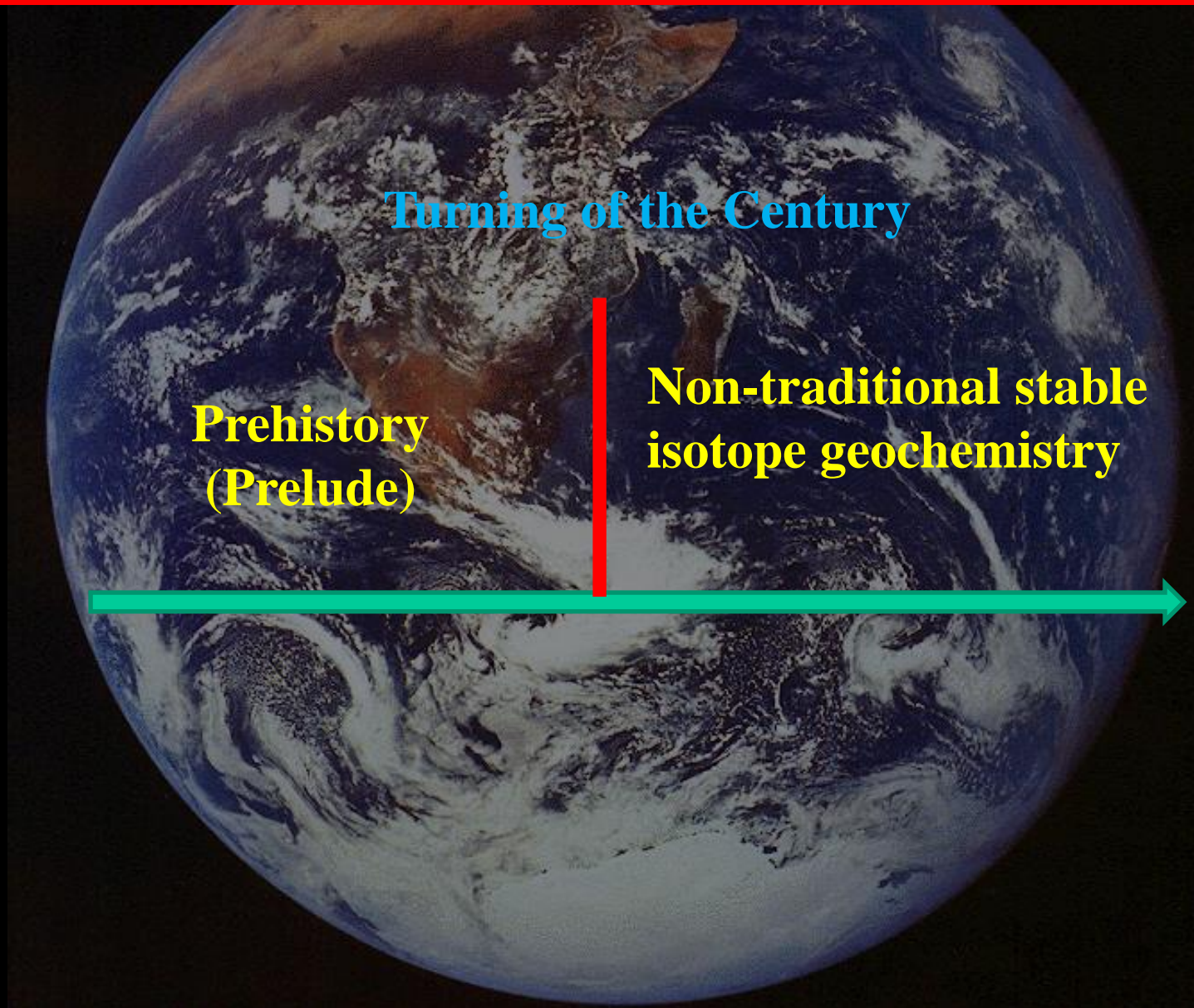
Possibly essential trace elements for some species

Why Non-traditional Isotopes?

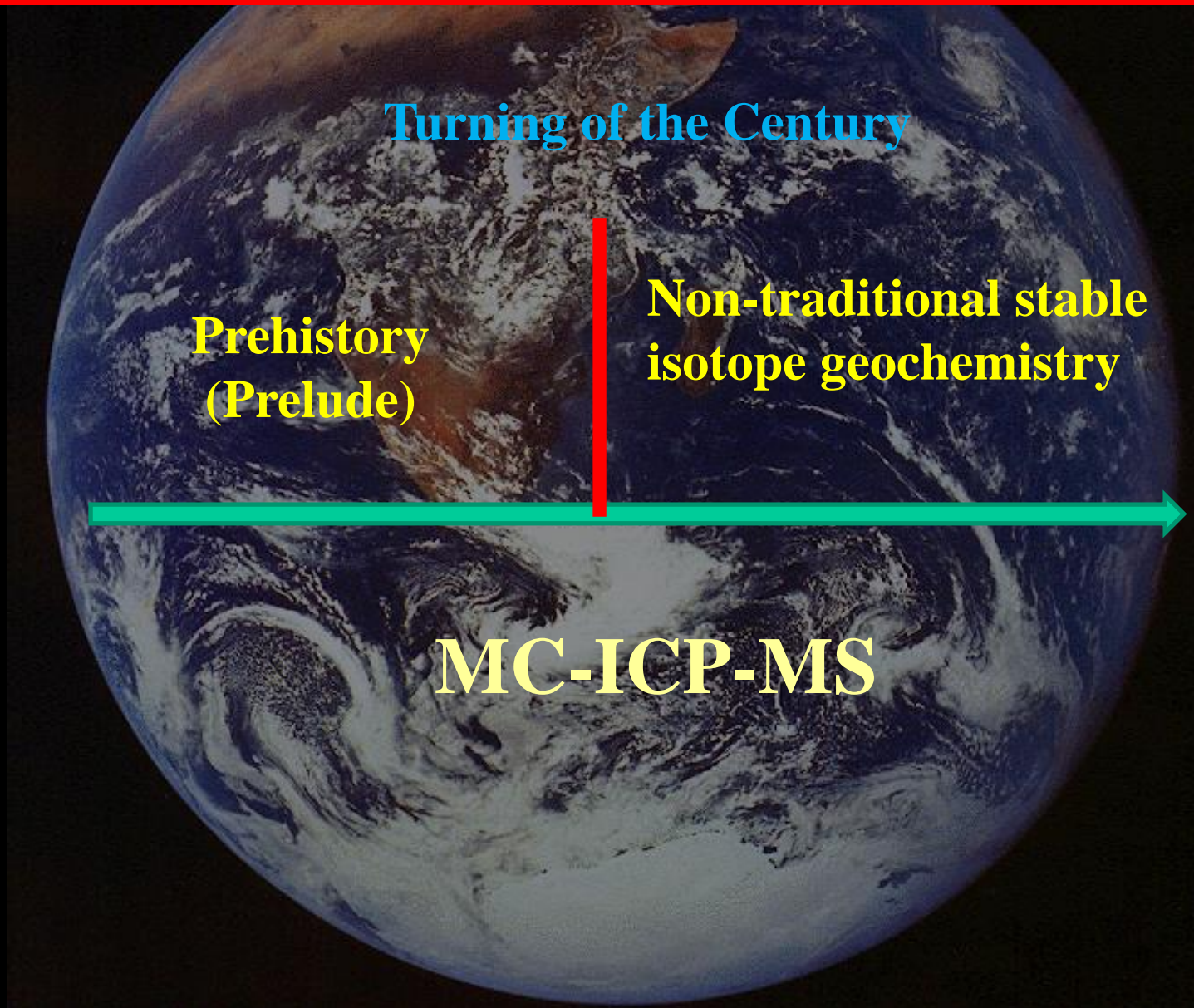
- **Biochemistry**
- Biologically utilised: Fe, Cu, Zn, Mo, Ca, Mg, etc.
- Biosphere-Geosphere interreaction



A brief history



A brief history



多接收器等离子体质谱仪 MC-ICP-MS



17 3:53 PM



热电离质谱仪
(TIMS)



气质质谱仪

MC-ICP-MS



Nu Plasma HR

26 5:2



高温等离子体，7000K，极高的电离效率；

多个接收器对信号同时接收，获得高精度同位素比值；

仪器的质量歧视相对稳定

Prehistory

- Cu isotopes (Shields et al., 1965)
- Zn isotopes (Blix et al., 1957; Rosman, 1972)
- Fe isotopes (Taylor et al., 1992)
- **No isotopic variations of natural materials have been detected (ca. 1%)**



BUG OFF !

Prehistory

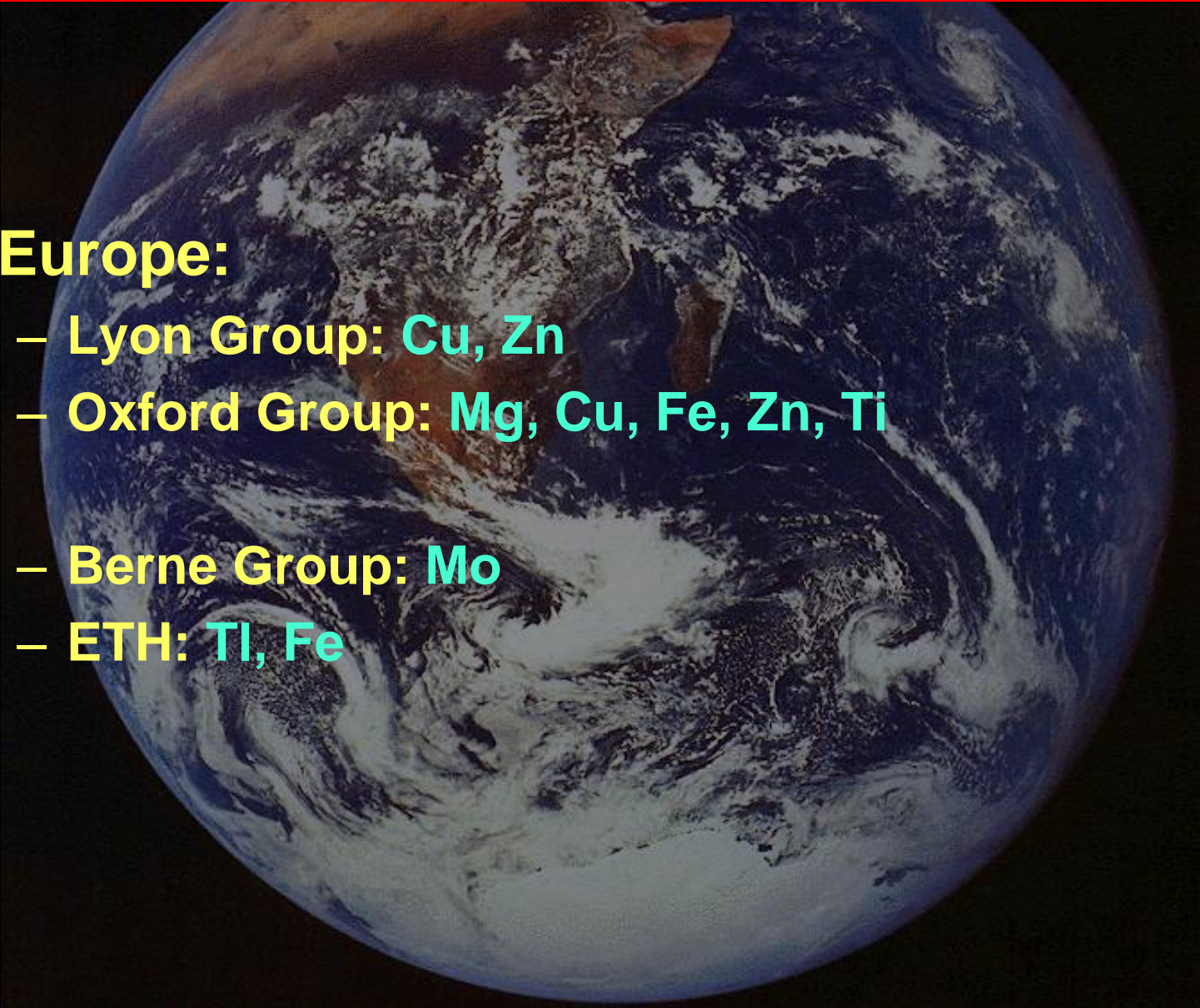
- Li isotopes (Chan, 1987);
 - B isotopes (Spivack and Edmond, 1986; Xiao et al., 1988)
 - Ca isotopes (Russell et al., 1977; Skulan et al., 1997)
 - **Slow developments**
- 

多接收器等离子体质谱仪 MC-ICP-MS



The beginning

- **Europe:**
 - Lyon Group: Cu, Zn
 - Oxford Group: Mg, Cu, Fe, Zn, Ti
 - Berne Group: Mo
 - ETH: Ti, Fe



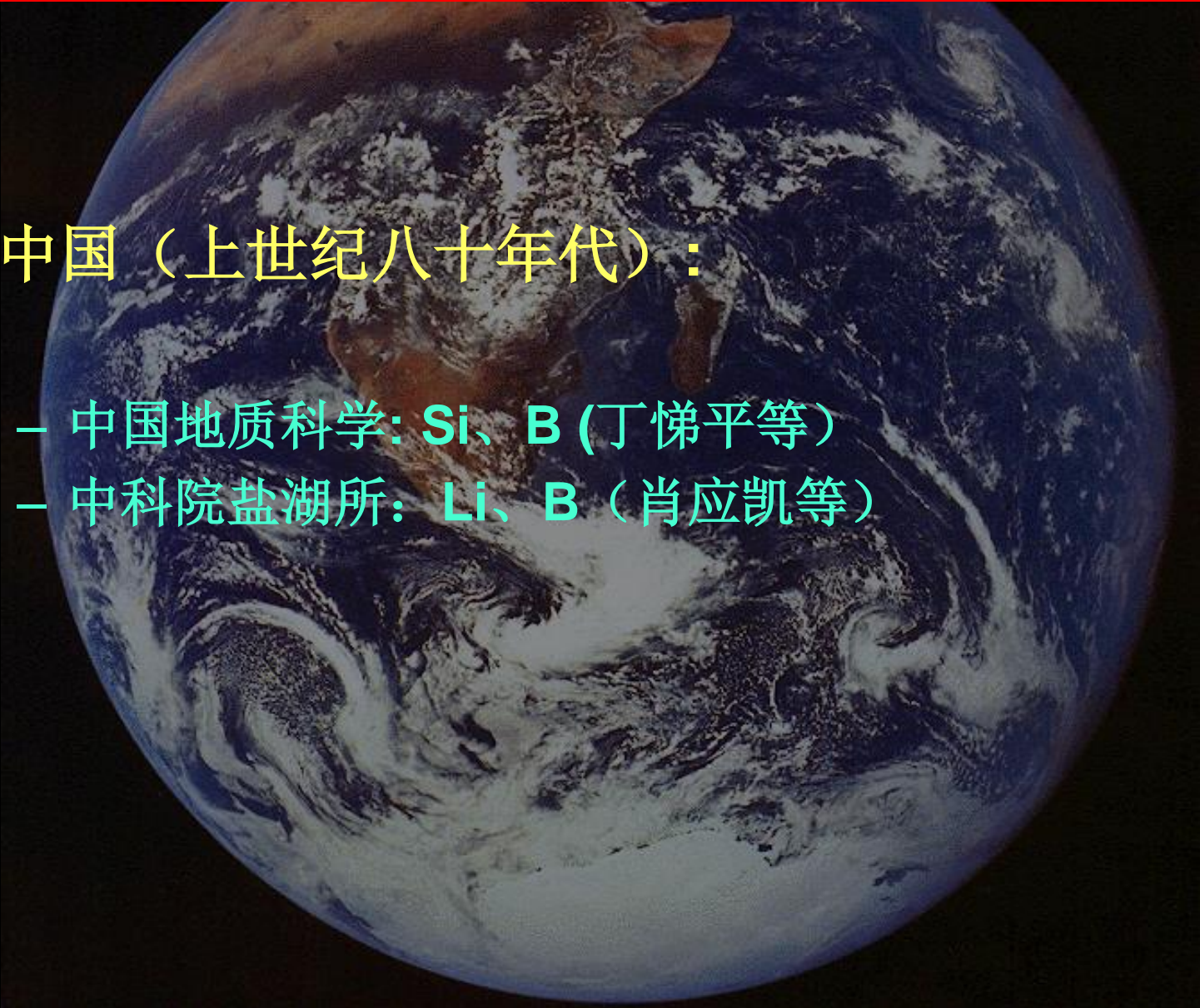
The beginning

- **USA:**
 - Clark Johnson Group: Fe
 - Tom Johnson: Cr, Se
 - Ariel Anbar Group: Mo



The beginning

- 中国（上世纪八十年代）：
 - 中国地质科学: **Si**、**B** (丁悌平等)
 - 中科院盐湖所: **Li**、**B** (肖应凯等)



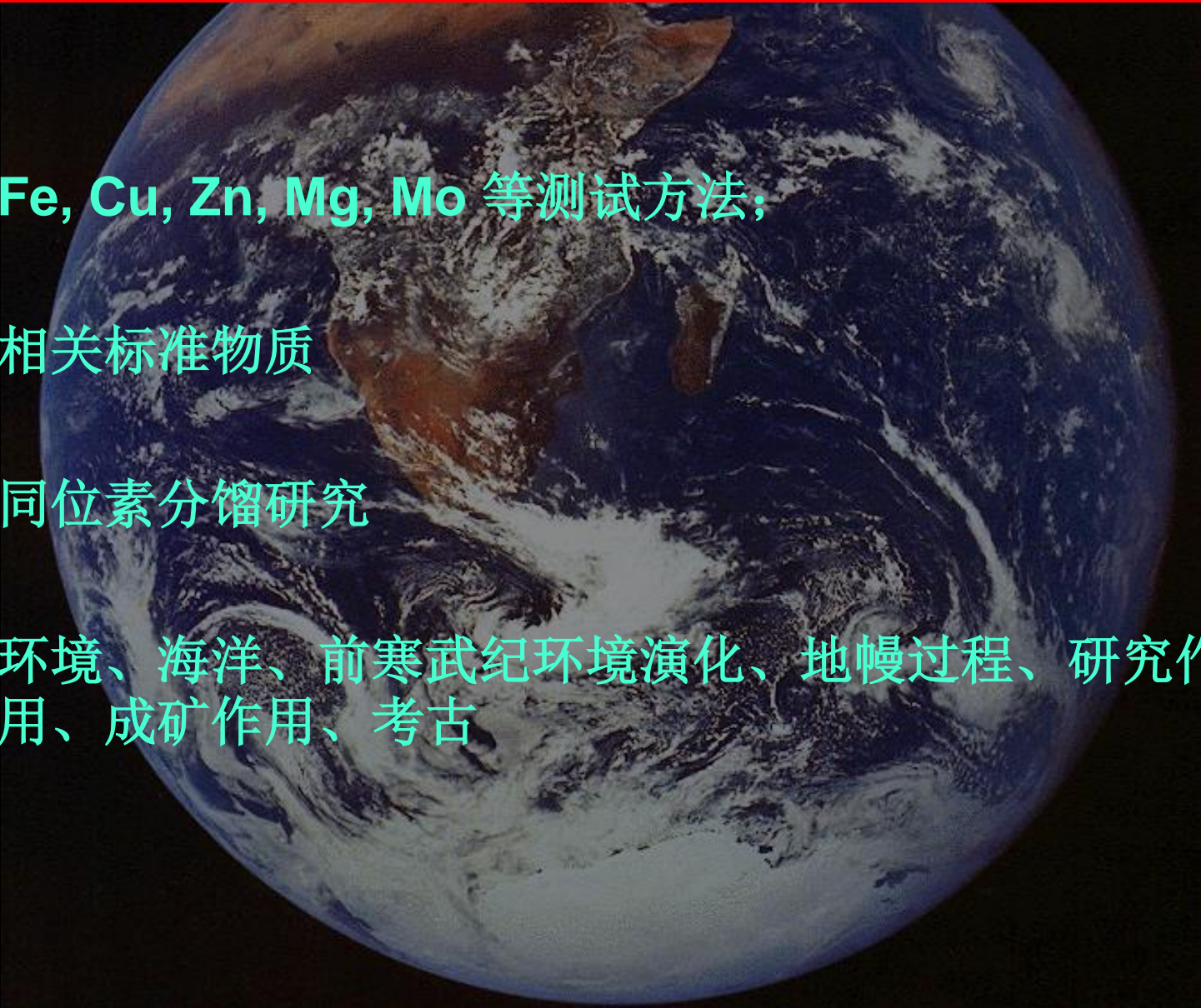
The beginning

- 中国:
 - 国土资源部同位素地质重点实验室:
2003年建立非传统稳定同位素分析研究实验室



The beginning

- Fe, Cu, Zn, Mg, Mo 等测试方法;
- 相关标准物质
- 同位素分馏研究
- 环境、海洋、前寒武纪环境演化、地幔过程、研究作用、成矿作用、考古



The beginning

- 中国科学院地球化学研究所
- 中国科学院广州地球化学研究所
- 中国科学院地质与地球物理研究所
- 西北大学
- 南京大学
- 中国地质大学（北京）
- 中国地质大学（武汉）
- 中国科技大学

The beginning

- 一批学者利用国外实验室开展研究;
- 一批学者学成回国。



几篇早期代表性论文



Pergamon

Geochimica et Cosmochimica Acta, Vol. 63, No. 11/12, pp. 1653–1660, 1999

Copyright © 1999 Elsevier Science Ltd

Printed in the USA. All rights reserved

0016-7037/99 \$20.00 + .00

PII S0016-7037(99)00089-7

High precision iron isotope measurements of terrestrial and lunar materials

BRIAN L. BEARD* and CLARK M. JOHNSON

Department of Geology and Geophysics, University of Wisconsin-Madison, Madison, Wisconsin 53706, USA

(Received August 5, 1998; accepted in revised form February 11, 1999)

Abstract—We present the analytical methods that have been developed for the first high-precision Fe isotope analyses that clearly identify naturally-occurring, mass-dependent isotope fractionation. A double-spike approach is used, which allows rigorous correction of instrumental mass fractionation. Based on 21 analyses of an ultra pure Fe standard, the external precision (1-SD) for measuring the isotopic composition of Fe is ± 0.14 ‰/mass; for demonstrated reproducibility on samples, this precision exceeds by at least an order of magnitude that of previous attempts to empirically control instrumentally-produced mass fractionation (Dixon et al., 1993). Using the double-spike method, 15 terrestrial igneous rocks that range in composition from peridotite to rhyolite, 5 high-Ti lunar basalts, 5 Fe-Mn nodules, and a banded iron formation have been analyzed for their iron isotopic composition. The terrestrial and lunar igneous rocks have the same isotopic compositions as the ultra pure Fe standard, providing a reference Fe isotope composition for the Earth and Moon. In contrast, Fe-Mn nodules and a sample of a banded iron formation have iron isotope compositions that vary over a relatively wide range, from $\delta^{56}\text{Fe} = +0.9$ to -1.2 ‰; this range is 15 times the analytical errors of our technique. These natural isotopic fractionations are interpreted to reflect biological (“vital”) effects, and illustrate the great potential Fe isotope studies have for studying modern and ancient biological processes. Copyright © 1999 Elsevier Science Ltd

DS-TIMS

REPORTS

the maximum insolation anomaly), and this age is used here. The third point (90.7 m) refers to the decline of Mediterranean elements and is assigned an age of 122.6 ka (event 5.51 of the SPECMAP time scale) on the basis of joint pollen and isotopic data from marine cores (23). Finally, the uppermost point (83.2 m), after which NAP percentages begin to exceed 50%, represents the transition from the last

interglacial to the ensuing stadial and is assigned an age for the MIS 5e/5d boundary of ~116 ka (22).

26. We thank R. C. Preece, T. C. Atkinson, and M. R. Chapman for comments and S. Boreham and H. Sloane for technical advice and assistance. We are grateful to the director-general and the staff at the Department of Energy Resources of the Institute of Geology and Mineral Exploration in Athens (particu-

Iron Isotope Biosignatures

Brian L. Beard,^{1*} Clark M. Johnson,¹ Lea Cox,² Henry Sun,²
Kenneth H. Nealson,² Carmen Aguilar³

The $^{56}\text{Fe}/^{54}\text{Fe}$ of Fe-bearing phases precipitated in sedimentary environments varies by 2.5 per mil ($\delta^{56}\text{Fe}$ values of +0.9 to -1.6 per mil). In contrast, the $^{56}\text{Fe}/^{54}\text{Fe}$ of Fe-bearing phases in igneous rocks from Earth and the moon does not vary measurably ($\delta^{56}\text{Fe} = 0.0 \pm 0.3$ per mil). Experiments with dissimilatory Fe-reducing bacteria of the genus *Shewanella algae* grown on a ferrihydrite substrate indicate that the $\delta^{56}\text{Fe}$ of ferrous Fe in solution is isotopically lighter than the ferrihydrite substrate by 1.3 per mil. Therefore, the range in $\delta^{56}\text{Fe}$ values of sedimentary rocks may reflect biogenic fractionation, and the isotopic composition of Fe may be used to trace the distribution of microorganisms in modern and ancient Earth.



Astrobiology

Unique biosignatures

LETTERS

Martian life?

Are the "very small" objects found on a Martian meteorite too small to be living organisms? (Right, a tube-like structural form 0.5 micrometers long.) If traces of earlier life on that planet have really been found, then what are some of the implications for theories about the origins of life? On other matters, progress in the use of insect-resistant transgenic plants is assessed. And research on how the human immunodeficiency virus fuses to the cell is discussed.



RESEARCH ARTICLE

Search for Past Life on Mars: Possible Relic Biogenic Activity in Martian Meteorite ALH84001

David S. McKay, Everett K. Gibson Jr.,
Kathie L. Thomas-Keprta, Hojatollah Vali,
Christopher S. Romanek, Simon J. Clemett,
Xavier D. F. Chillier, Claude R. Maechling, Richard N. Zare



Fe isotopes are heavy enough cannot to be fractionated inorganically

But light enough to be fractionated biologically

REPORTS

Nonbiological Fractionation of Iron Isotopes

A. D. Anbar,^{1,2*} J. E. Roe,² J. Barling,¹ K. H. Nealson³

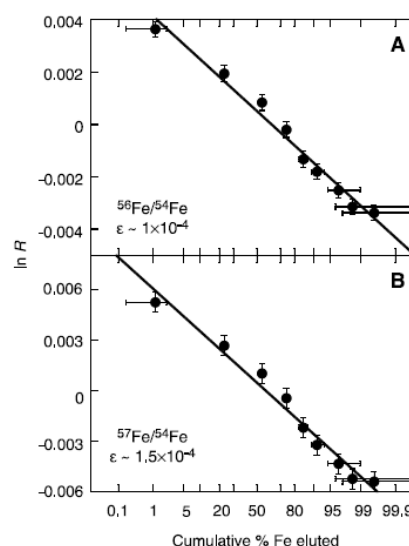
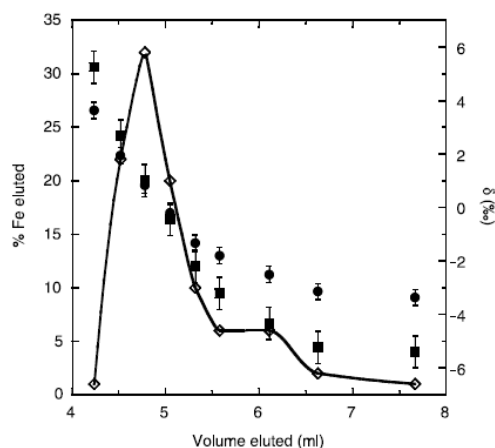
Laboratory experiments demonstrate that iron isotopes can be chemically fractionated in the absence of biology. Isotopic variations comparable to those seen during microbially mediated reduction of ferrihydrite are observed. Fractionation may occur in aqueous solution during equilibration between inorganic iron complexes. These findings provide insight into the mechanisms of iron isotope fractionation and suggest that nonbiological processes may contribute to iron isotope variations observed in sediments.

variations result from mass-dependent fractionation rather than from isobaric interferences. We find $\delta^{56}\text{Fe} \sim 0.68 \times \delta^{57}\text{Fe}$ ($r^2 = 0.99$), which is consistent with theory (21). Additional verification is provided by mass balance, which requires that the isotopic composition of the eluted Fe integrated over all elution fractions should be identical to that of the loaded Fe if 100% of the loaded Fe is recovered. This expectation is confirmed in our system, where $\delta^{56}\text{Fe}$ and $\delta^{57}\text{Fe}$ are ~ 0 when the cumulative yield is $\sim 100\%$.

Chromatographic data can be related to $^{54}\text{K}_D/^{56}\text{K}_D$ and $^{54}\text{K}_D/^{57}\text{K}_D$ by recognizing that the $\delta^{56}\text{Fe}$ and $\delta^{57}\text{Fe}$ data reflect the superposition of these independent elution curves.

REPORTS

Fig. 1 (left). $\delta^{56}\text{Fe}$ (●) and $\delta^{57}\text{Fe}$ (■) versus volume eluted in a typical chromatographic experiment (15). For Fe loaded on the column, $\delta^{56}\text{Fe} = \delta^{57}\text{Fe} \equiv 0\text{‰}$. (◇) percent of total Fe recovered in each fraction; the cumulative yield was 100%. Integrated over all elution fractions, cumulative $\delta^{56}\text{Fe} = 0.2 \pm 0.3\text{‰}$ and cumulative $\delta^{57}\text{Fe} = 0.0 \pm 0.6\text{‰}$. Error bars indicate $\pm 2\sigma$ uncertainties. Fig. 2 (right). Isotopic compositions in chromatographic elution fractions (R) plotted against cumulative percent Fe recovered on a probability abscissa (17, 18). $R = (^M\text{Fe}/^{54}\text{Fe})_{\text{fraction}} / (^M\text{Fe}/^{54}\text{Fe})_{\text{total}}$, where $M = 56$ (A) or 57 (B). The slope on such plots reflects the extent of isotope separation during elution, and is approximately equal to $-\varepsilon/\sqrt{N}$. N , the number of theoretical plates in the column (28); ε , the single-step ("batch") enrichment factor (17, 18). If isotope separation is the result of equilibration with the resin, $^{54}\text{K}_D/^{56}\text{K}_D = 1 + \varepsilon$. Error bars indicate $\pm 2\sigma$ uncertainties.



Precise analysis of copper and zinc isotopic compositions by plasma-source mass spectrometry

Chloé Nadia Maréchal ^{*}, Philippe Télouk, Francis Albarède

*Laboratoire de Sciences de la Terre (Unité Mixte de Recherche CNRS 8515), Ecole Normale Supérieure de Lyon, 46 Allée d'Italie, 69364
Lyon, Cedex 07, France*

Received 6 July 1998; accepted 30 October 1998



**First paper for non-traditional stable isotope
measurements using MC-ICPMS**
Element-doping



ELSEVIER

Chemical Geology 163 (2000) 139–149

**CHEMICAL
GEOLOGY**

INCLUDING
ISOTOPE GEOSCIENCE

www.elsevier.com/locate/chemgeo

Determination of natural Cu-isotope variation by plasma-source mass spectrometry: implications for use as geochemical tracers

X.K. Zhu ^{a,*}, R.K. O’Nions ^a, Y. Guo ^a, N.S. Belshaw ^a, D. Rickard ^b

^a *Department of Earth Sciences, University of Oxford, Parks Road, Oxford, OX1 3PR UK*

^b *Department of Earth Sciences, University of Wales, Cardiff, CF1 3YE UK*

Received 21 December 1998; accepted 29 April 1999

First report for non-traditional stable isotope measurements using standard-sample-bracketing techniques

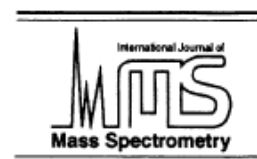
Secular Variation of Iron Isotopes in North Atlantic Deep Water

Xiang-Kun Zhu,* R. Keith O'Nions, Yueling Guo, Ben C. Reynolds

A high-precision iron isotope time series for a ferromanganese crust demonstrates that the iron isotope composition in North Atlantic Deep Water has



ELSEVIER



International Journal of Mass Spectrometry 197 (2000) 191–195

High precision measurement of iron isotopes by plasma source mass spectrometry

N.S. Belshaw, X.K. Zhu, Y. Guo, R.K. O'Nions

Department of Earth Sciences, University of Oxford, Parks Road, Oxford OX1 3PR, UK

Received 2 July 1999; accepted 15 October 1999

Isotopic homogeneity of iron in the early solar nebula

X. K. Zhu, Y. Guo, R. K. O'Nions, E. D. Young & R. D. Ash

Department of Earth Sciences, University of Oxford, Parks Road, Oxford OX1 3PR, UK

present the results of measurements of the $^{56}\text{Fe}/^{54}\text{Fe}$ and $^{57}\text{Fe}/^{54}\text{Fe}$ ratios in terrestrial and extraterrestrial materials.

We have sampled a wide variety of meteorite types, representing different parent bodies. These include chondrites (carbonaceous, ordinary, and enstatite chondrites), achondrites (aubrite, eucrite, ureilite, and Shergotty–Nakhla–Chassigny (SNC) meteorite), pallasites, and iron meteorites. We performed measurements of iron isotopes on chondrules, matrices, metal fractions, or bulk samples. Chondrules were hand-picked from the meteorites after gentle crushing, and freed from matrix coating by air abrasion and

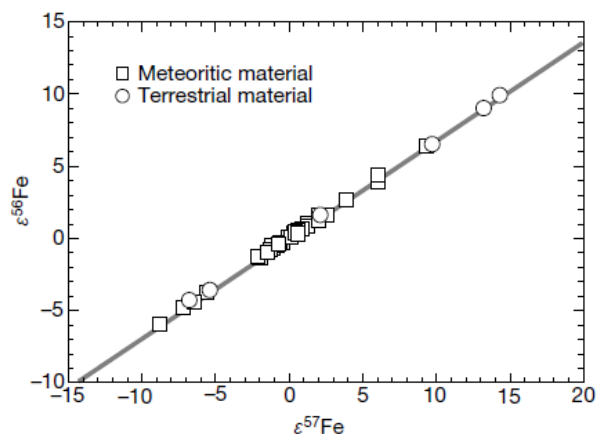


Figure 1 A three-isotope plot for iron, showing that all the Fe-isotope data from both terrestrial and extraterrestrial materials plot on a single mass-fractionation line. The correlation between $\epsilon^{56}\text{Fe}$ and $\epsilon^{57}\text{Fe}$ is $\epsilon^{56}\text{Fe} = (0.677 \pm 0.004)\epsilon^{57}\text{Fe}$, and $r^2 = 0.999$. If the regression is not forced through the origin, then $\epsilon^{56}\text{Fe} = (0.678 \pm 0.004)\epsilon^{57}\text{Fe} - 0.034$, with $r^2 = 0.999$. The size of data points represents the analytical uncertainty, which is defined as two standard deviations of long-term repeatability.

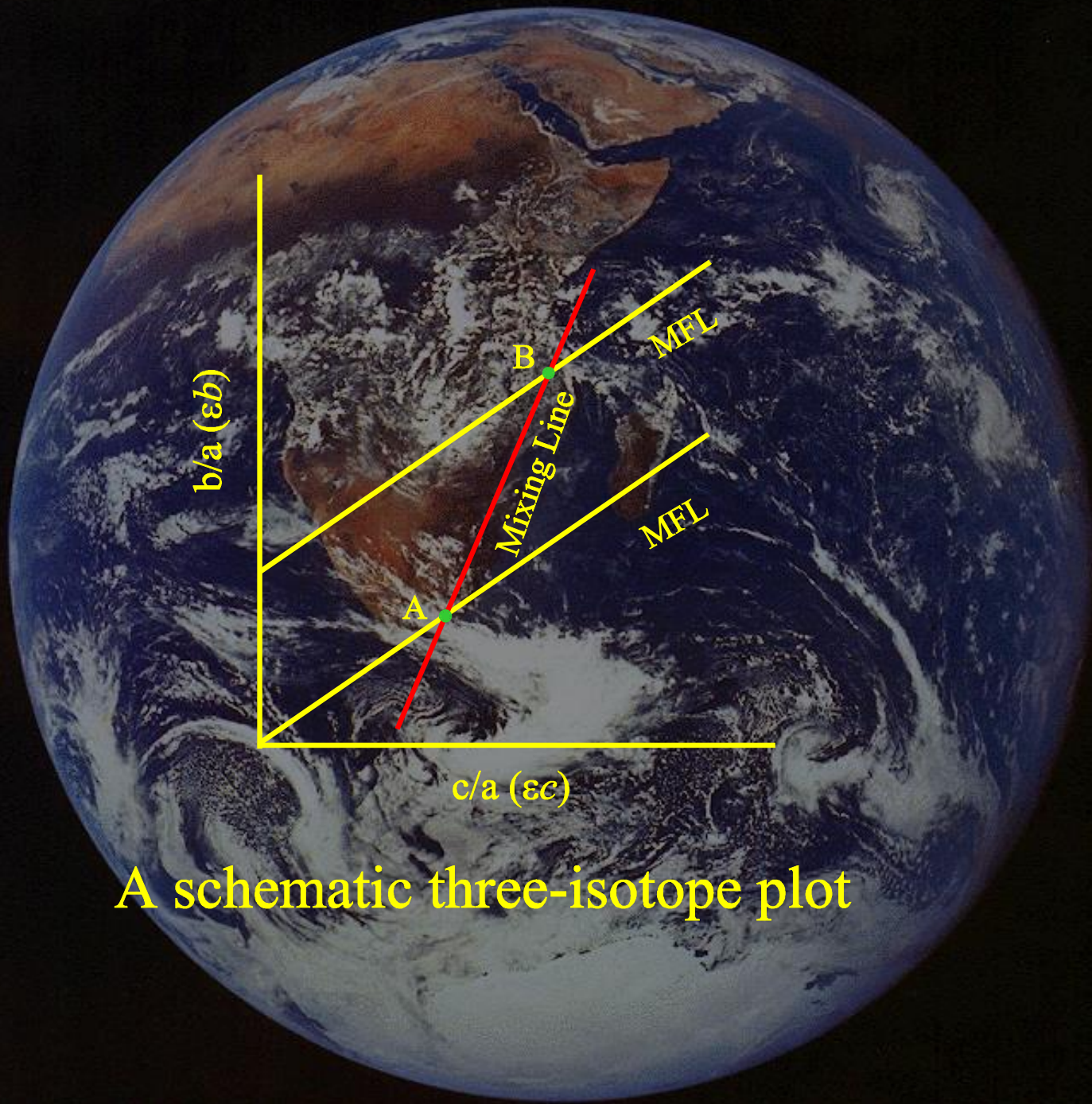
Constraints on the homogeneity of the early solar nebula

- The degree of chemical & isotopic homogeneity of the solar nebula is a basic issue in the study of solar system evolution;
- Variations in three or more isotopes of an element can constrain this issue;

蟹状星云

Elements are synthesized in stars

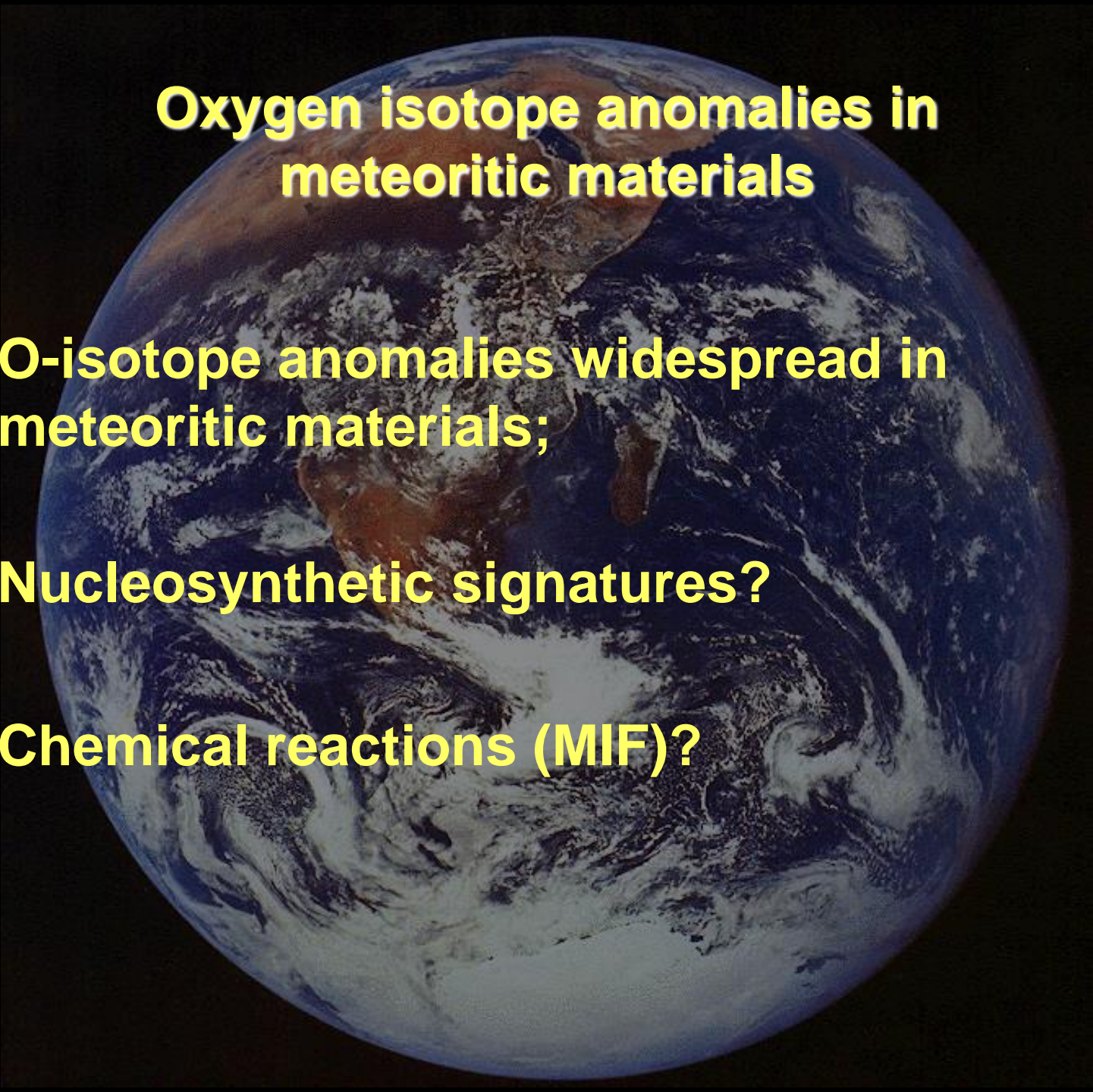
**different stars produce elements with
different proportions of isotopes**



A schematic three-isotope plot

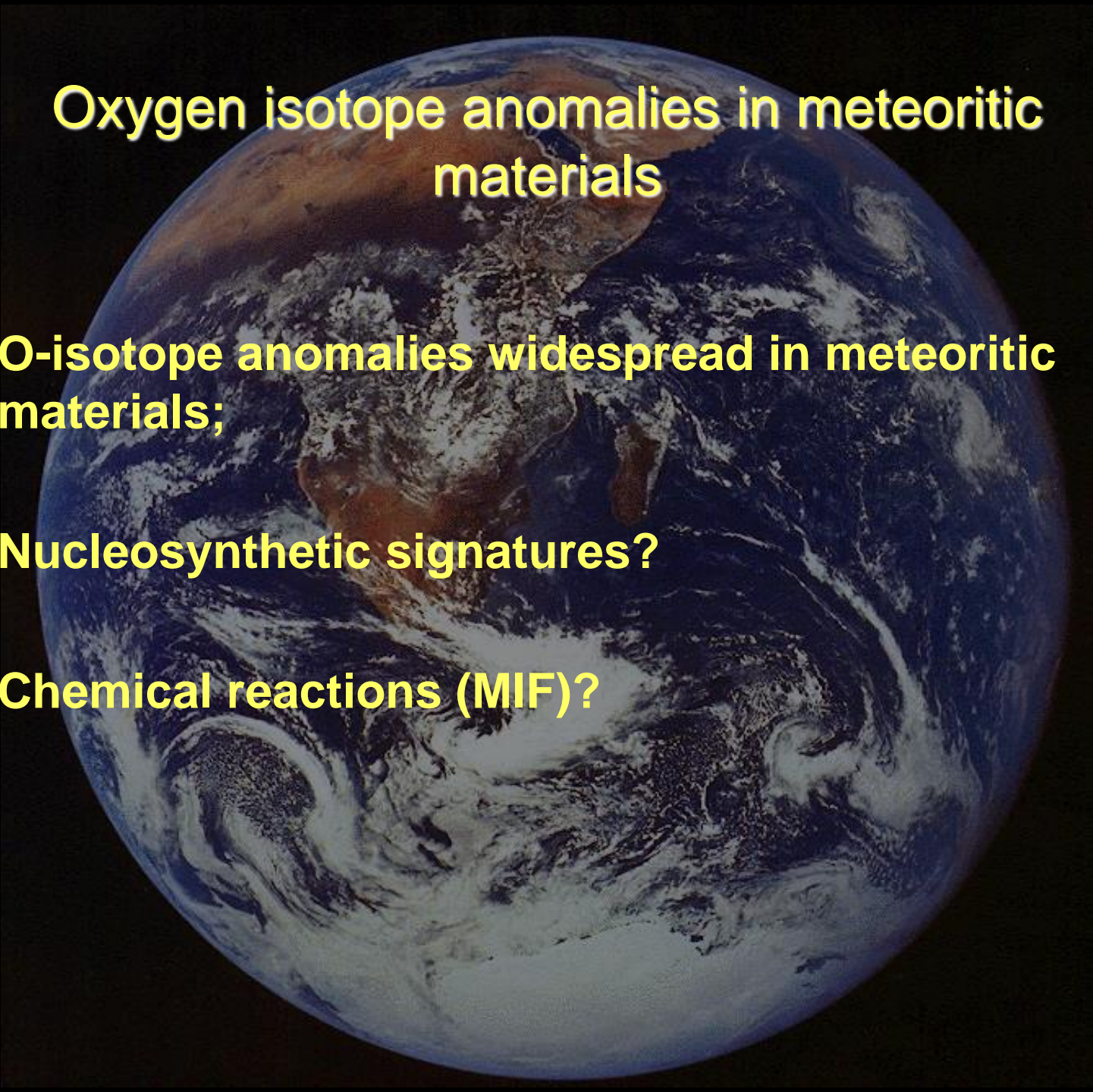
Oxygen isotope anomalies in meteoritic materials

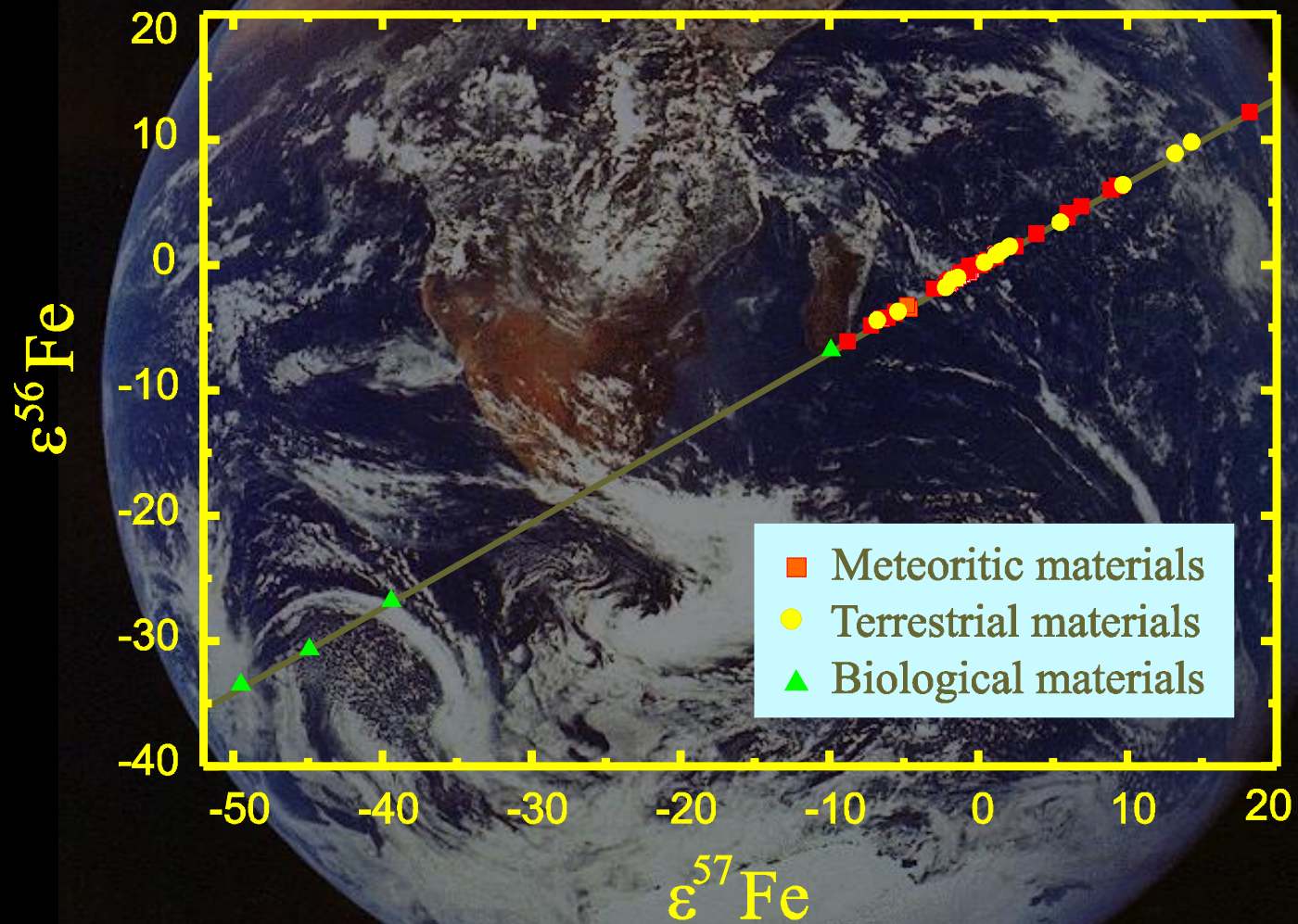
- **O-isotope anomalies widespread in meteoritic materials;**
- **Nucleosynthetic signatures?**
- **Chemical reactions (MIF)?**

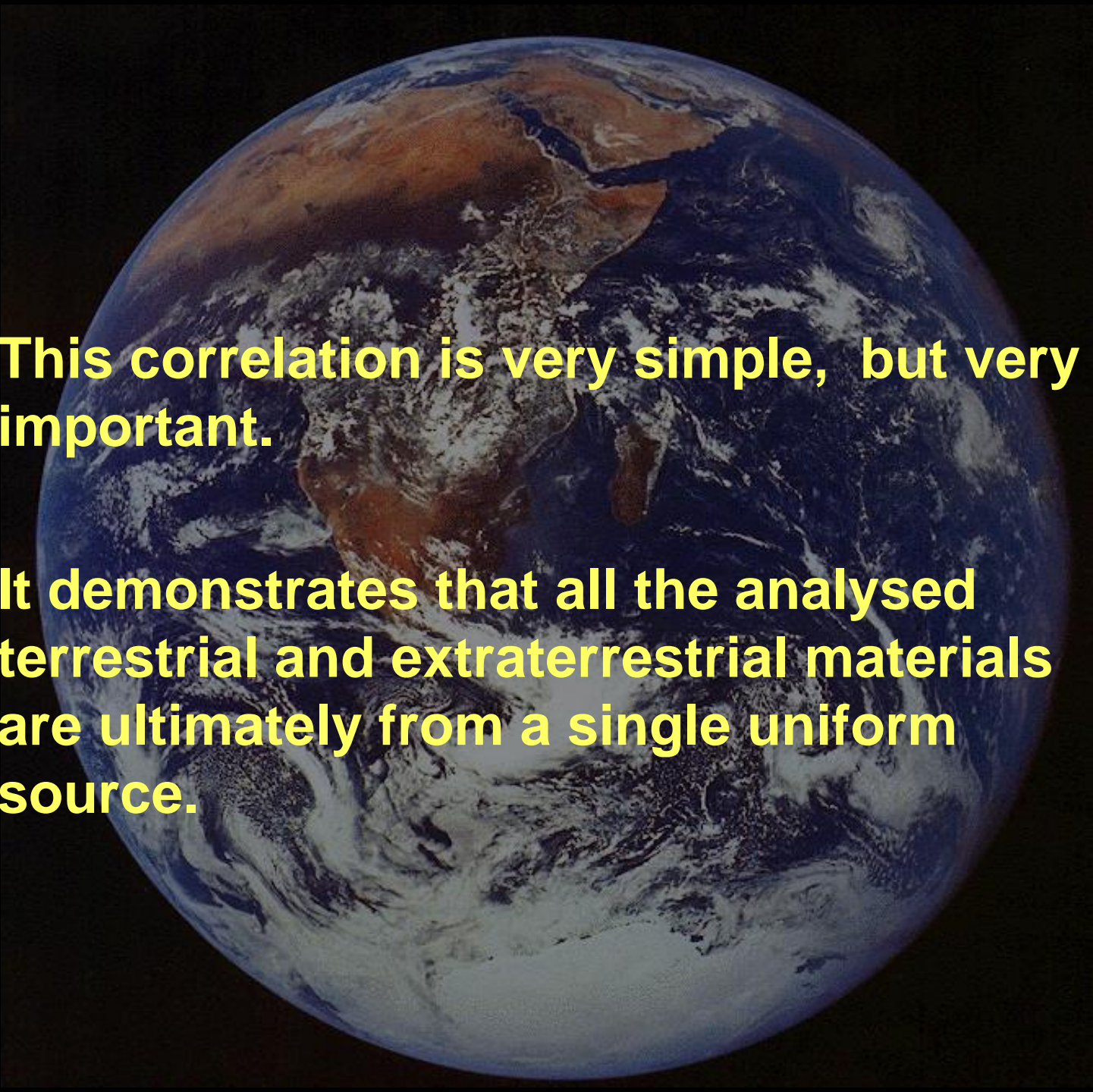


Oxygen isotope anomalies in meteoritic materials

- O-isotope anomalies widespread in meteoritic materials;
- Nucleosynthetic signatures?
- Chemical reactions (MIF)?





- 
- **This correlation is very simple, but very important.**
 - **It demonstrates that all the analysed terrestrial and extraterrestrial materials are ultimately from a single uniform source.**

Mass fractionation processes of transition metal isotopes

X.K. Zhu^{a,*}, Y. Guo^a, R.J.P. Williams^b, R.K. O’Nions^a, A. Matthews^{a,c},
N.S. Belshaw^a, G.W. Canters^d, E.C. de Waal^d, U. Weser^e, B.K. Burgess^{f,1},
B. Salvato^g

^a *Department of Earth Sciences, University of Oxford, Parks Road, Oxford OX1 3PR, UK*

^b *Department of Chemistry, University of Oxford, South Parks Road, Oxford OX1 3QR, UK*

^c *Institute of Earth Sciences, Hebrew University of Jerusalem, 91904 Jerusalem, Israel*

^d *Leiden Institute of Chemistry, Leiden University, Einsteinweg 55, 2333 CC Leiden, The Netherlands*

^e *Anorganische Biochemie, Physiologisch-Chemische Institut, Eberhard-Karls-Universität Tübingen, Hoppe-Seyler-Str. 4,
D-72076 Tübingen, Germany*

^f *Department of Molecular Biology and Biochemistry, University of California, Irvine, CA 92717, USA*

^g *CNR Centre of Metalloproteins, Padua University, I-35121 Padua, Italy*

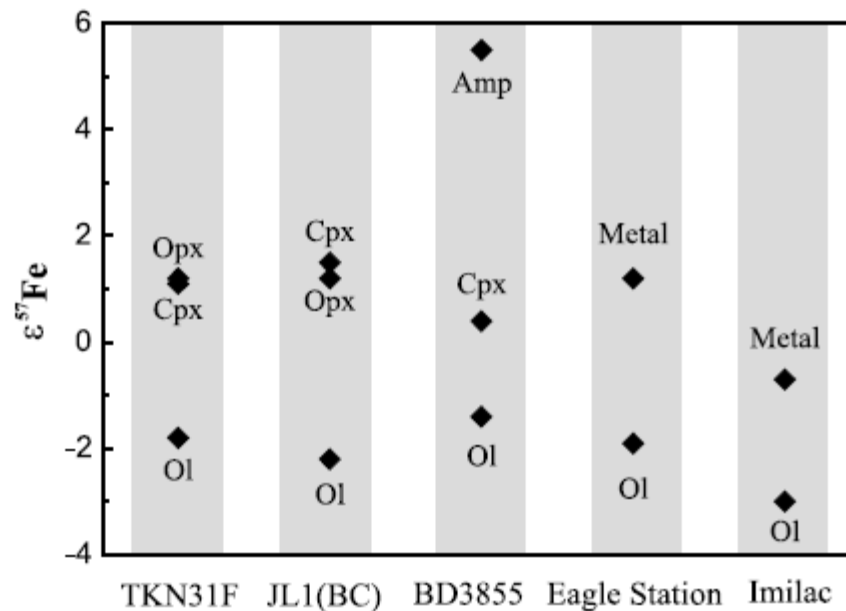
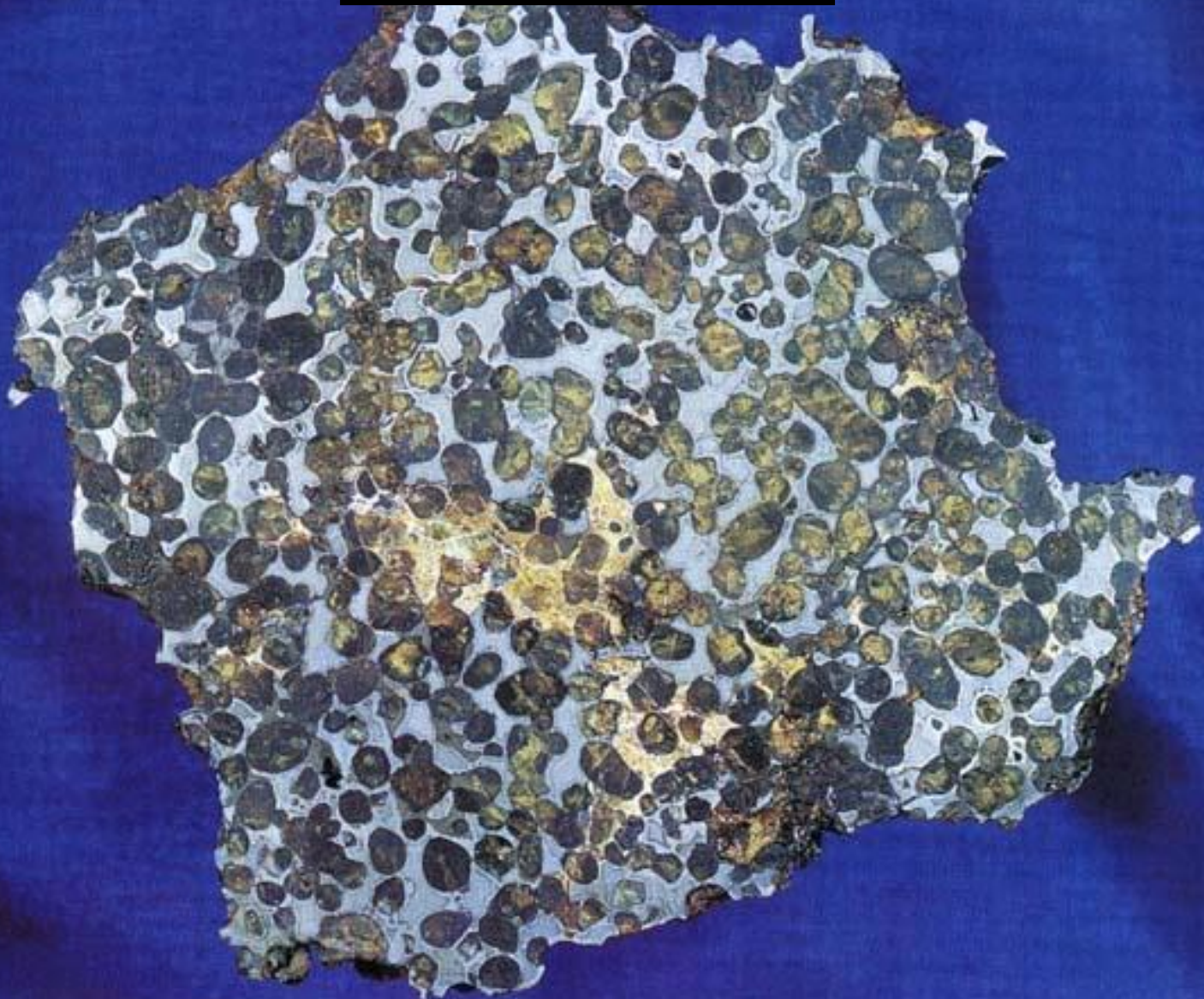


Fig. 1. A plot showing phase-related variation of Fe isotopes in mantle xenoliths and pallasites. All results for $\epsilon^{57}\text{Fe}$ are relative to IRMM-14 standard. The size of data symbols represents approximately the external precision at 1σ level. Ol-olivine; Opx-orthopyroxene; Cpx-clinopyroxene; Amp-amphibole.

Pallasite



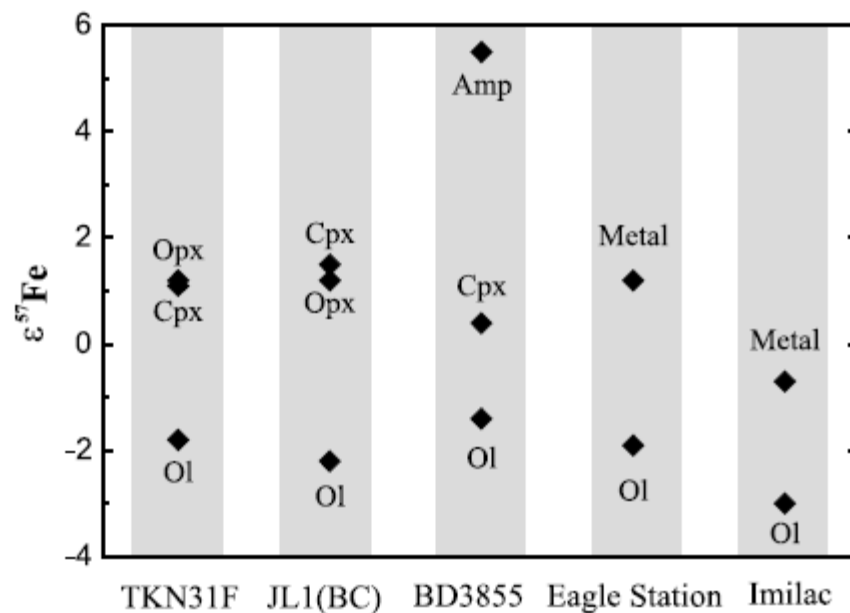


Fig. 1. A plot showing phase-related variation of Fe isotopes in mantle xenoliths and pallasites. All results for $\epsilon^{57}\text{Fe}$ are relative to IRMM-14 standard. The size of data symbols represents approximately the external precision at 1 σ level. Ol-olivine; Opx-orthopyroxene; Cpx-clinopyroxene; Amp-amphibole.

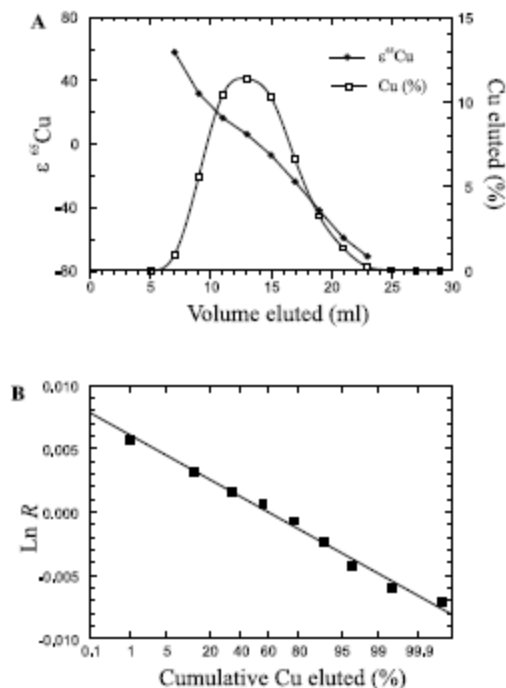


Fig. 2. Equilibrium mass fractionation of Cu isotopes between aqueous species during ion exchange chromatography. (A) $\epsilon^{65}\text{Cu}$ values for Cu eluted from an ion exchange column using anion resin AG-MP1. The overall isotope fractionation that occurred during the chromatographic process is considered to result from multiple step equilibrium fractionation between the resin bound CuCl_4^{2-} and the free CuCl_2^0 species. From an ideal Gaussian elution curve, the number of steps (i.e., the number of theoretical plates), N , is obtained from the relation $N = 5.54 \times (V_R/W_{1/2})^2$ where V_R is the volume to the curve peak and $W_{1/2}$ is the width of the curve at half-height [27]. If the tailing effect is neglected, then $N=12$. (B) Cu isotope compositions in elution fractions, R , vs. cumulative percentage of Cu eluted on a normal deviate (probability) scale. $R = (^{65}\text{Cu}/^{63}\text{Cu})_{\text{fraction}} / (^{65}\text{Cu}/^{63}\text{Cu})_{\text{initial}}$. The slope b on such a plot reflects the extent of isotope separation during elution, and $b \approx -\beta\sqrt{N}$, where N is the number of theoretical plates in the column, and β is the enrichment factor per single plate [29]. The line represents a best visual fit to the data.

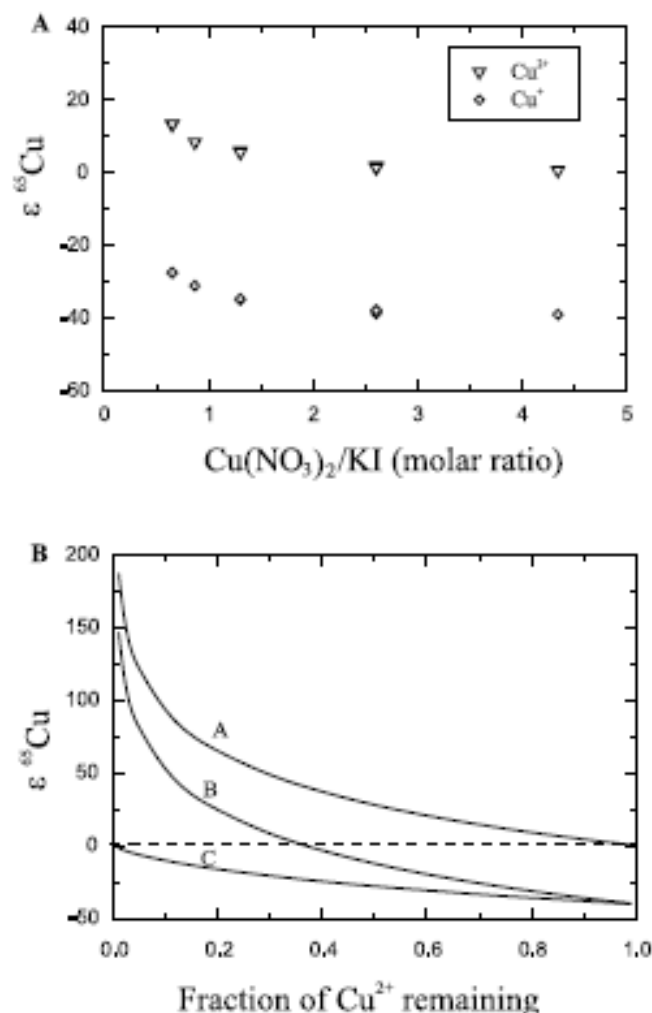


Fig. 3. (A) Experimental results of Cu isotope fractionation between Cu^{2+} and Cu^{+} aqueous species at 20°C . All $\epsilon^{65}\text{Cu}$ values are expressed relative to the original Cu solution used for the experiments. Note that the mass fractionation between Cu^{2+} solution and CuI precipitates remains constant at c. 40 ‰ units in $^{65}\text{Cu}/^{63}\text{Cu}$ ratio over a large range of experimental conditions. (B) Modelling results of Rayleigh fractionation between Cu^{2+} and Cu^{+} based on a fractionation factor between the two species $\alpha=1.00403$ as defined by the experimental results presented in panel A. Curve A is for $\epsilon^{65}\text{Cu}$ variation in the Cu^{2+} species remaining in solution. Curve B shows the variation of $\epsilon^{65}\text{Cu}$ in the CuI phase precipitated in equilibrium with Cu^{2+} aqueous species from the solution. Curve C shows the change of $\epsilon^{65}\text{Cu}$ in the accumulative CuI precipitate as a function of its accumulation. The dashed line represents the isotope composition of the initial solution. These results show three important points. Firstly, the heavy isotope enrichment in the remaining Cu^{2+} solution relative to the initial solution can be much larger than the equilibrium fractionation between Cu^{2+} and Cu^{+} species. Secondly, relative to the initial solution, both Cu^{2+} and Cu^{+} species can show heavy isotope enrichment. Thirdly, the overall fractionation between Cu^{2+} and Cu^{+} species can be much larger than the equilibrium fractionation between the two species.

tween the two Cu species at c. 20°C for the given experimental conditions, $\alpha_{\text{Cu(II)}-\text{Cu(I)}} = 1.00403 \pm 0.00004$, can be defined by the experiment results.

Using the fractionation factor obtained above, the significance of the results in understanding mass fractionation of transition metal isotopes during redox-related processes in natural systems

Table 3

Measurements of transition metal isotopes in biological samples

Sample	$\epsilon^{56}\text{Fe}^a$	$\epsilon^{57}\text{Fe}^a$	$\epsilon^{65}\text{Cu}^b$	$\epsilon^{66}\text{Zn}^c$	$\epsilon^{67}\text{Zn}^c$	$\epsilon^{68}\text{Zn}^c$
Ferredoxin-I expressed in <i>Azotobacter vinelandii</i>	-6.8	-9.9				
Culture solution after incubation	2.2	3.3				
FeCl_3 , source material	2.1	3.0				
Azurin expressed in <i>E. coli</i>			-16.4			
Azurin expressed in <i>P. aeruginosa</i>			-10.9			
$\text{Cu}(\text{NO}_3)_2$, source material			-1.1			
Yeast Cu-metallothionein			-21.3			
Yeast Cu-Zn-superoxide dismutase			-16.0	10.8	16.3	21.0
CuSO_4 , source material			-4.2			
Bovine haemoglobin	-26.8	-39.4				
Horse haemoglobin	-30.7	-44.9				
Pig haemoglobin	-33.5	-49.5				
Octopus haemocyanin			6.2			

^a Measured $^{57}\text{Fe}/^{54}\text{Fe}$ and $^{56}\text{Fe}/^{54}\text{Fe}$ ratios are expressed as $\epsilon^{57}\text{Fe}$ and $\epsilon^{56}\text{Fe}$, which are deviations in parts per 10^4 from the Fe isotope reference material IRMM-14. See footnote of Table 1 for data precision.

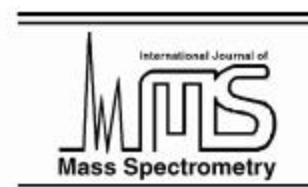
^b Measured $^{65}\text{Cu}/^{63}\text{Cu}$ ratio is expressed as $\epsilon^{65}\text{Cu}$, which is deviation in parts per 10^4 from the Cu isotope reference material NIST-976. See footnote of Table 2 for data precision.

^c Measured $^{66}\text{Zn}/^{64}\text{Zn}$, $^{67}\text{Zn}/^{64}\text{Zn}$ and $^{68}\text{Zn}/^{64}\text{Zn}$ ratios are expressed as $\epsilon^{66}\text{Zn}$, $\epsilon^{67}\text{Zn}$ and $\epsilon^{68}\text{Zn}$, which are deviations in parts per 10^4 from an Aldrich standard solution. Repeated measurements of Romil Zn solution versus Aldrich Zn solution over a period of a few months give external precision of 0.5, 0.5 and 0.6‰ at 2σ level for $\epsilon^{66}\text{Zn}$, $\epsilon^{67}\text{Zn}$ and $\epsilon^{68}\text{Zn}$, respectively.



ELSEVIER

International Journal of Mass Spectrometry 220 (2002) 21–29



www.elsevier.com/locate/ijms

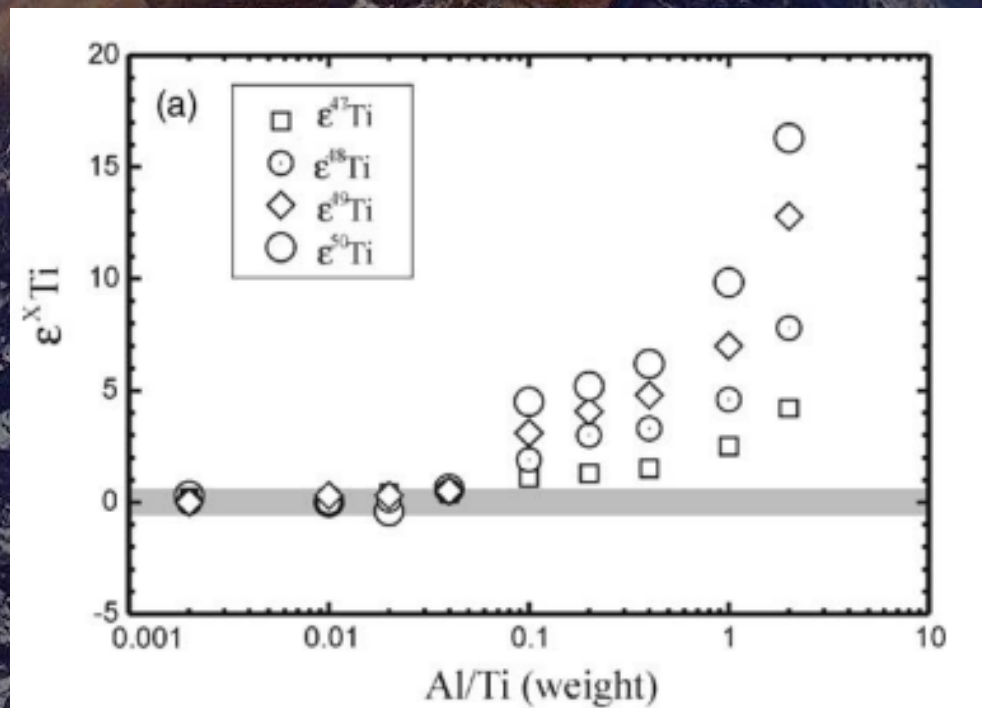
High precision measurement of titanium isotope ratios by plasma source mass spectrometry

X.K. Zhu^{a,b,*}, A. Makishima^{a,c}, Y. Guo^a, N.S. Belshaw^a, R.K. O’Nions^a

^a *Department of Earth Sciences, Oxford University, Parks Road, Oxford OX1 3PR, UK*

^b *Laboratory of Isotope Geochemistry and Cosmochemistry, Chinese Academy of Geological Sciences,
Baiwanzhuang Road 26, Beijing 100037, China*

^c *The Pheasant Memorial Laboratory for Geochemistry and Cosmochemistry, Institute for Study of the Earth’s Interior,
Okayama University at Misasa, Misasa, Tottori-ken 682-0193, Japan*



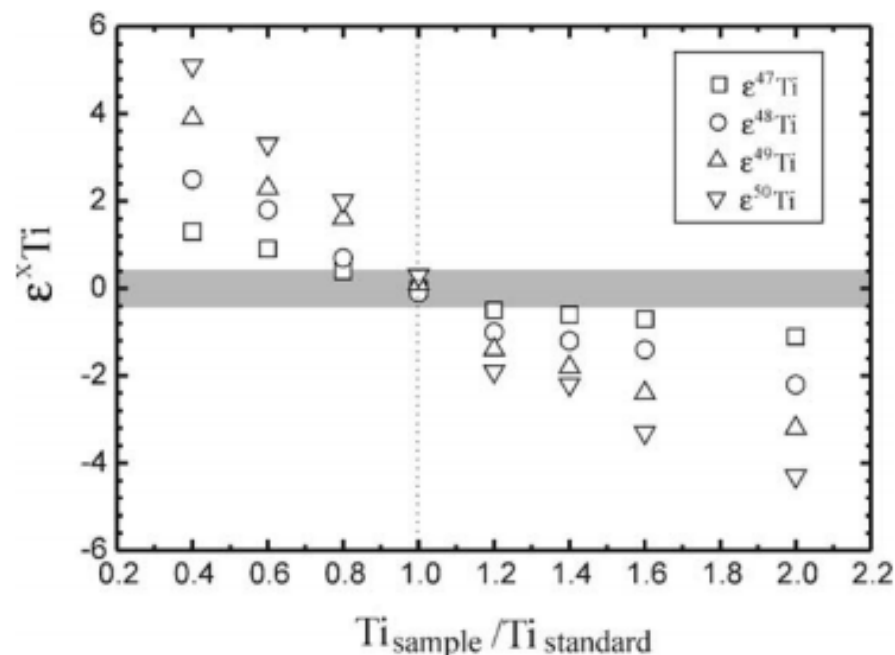
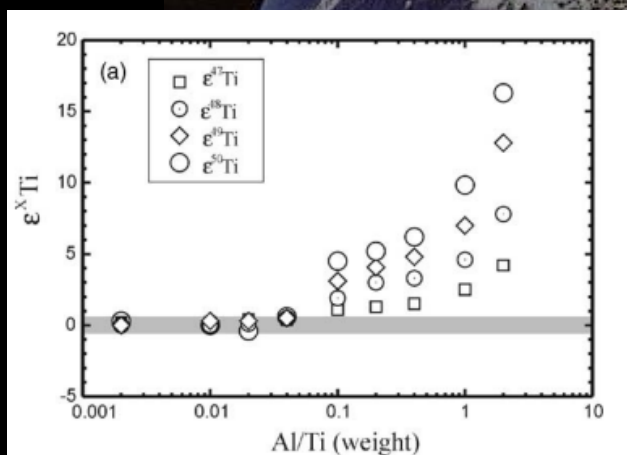


Fig. 2. A plot showing the effect of varying Ti concentration on the measured Ti isotope ratios. Unlike the interference effects shown in Fig. 1b, the variances of the measured Ti isotope ratios follow a mass-dependent manner. These results were obtained with the desolvating nebuliser running without N_2 gas. The width of the grey band represents the long-term repeatability of $\epsilon^{47}\text{Ti}$ at the 2 standard deviation level, as defined in Fig. 4. The dotted line represents the position where the Ti concentration of “sample” solution is the same as that of the standard. The Ti concentration of solution used as the standard in these experiments is 5 ppm.

of nearest neighbor molecules.

The present experiments give clear evidence that laser irradiation plays a fundamental role in the activation of the polymerization that prevails over the competing dimerization process. The obtainment of pure *trans*-polybutadiene is indeed a remarkable result. As a whole, the high-pressure reaction studied in the present report has several interesting features including the high selectivity of the process, the easy switching from one pathway to the other, and the full transformation into the product with the absence of solvents and catalysts, thus fulfilling several of the requirements for a green chemistry process (30).

References and Notes

1. H. G. Drickamer, *Science* **156**, 3779 (1967).
2. C. S. Yoo, M. Nicol, *J. Phys. Chem.* **90**, 6732 (1986).
3. K. Aoki, Y. Kakudate, M. Yoshida, S. Usuba, S. Fujiwara, *J. Chem. Phys.* **91**, 778 (1989).
4. M. Sakashita, H. Yamawaki, K. Aoki, *J. Phys. Chem.* **100**, 9943 (1996).
5. M. Ceppatelli, M. Santoro, R. Bini, V. Schettino, *J. Chem. Phys.* **113**, 5991 (2000).
6. Ph. Pruzan, J. C. Chervin, M. M. Thiery, J. P. Itie, J. M. Besson, *J. Chem. Phys.* **92**, 6910 (1990).
7. F. Carsell, D. Fabre, J. P. Petit, *J. Chem. Phys.* **99**, 7300 (1993).
8. L. Ciabini, M. Santoro, R. Bini, V. Schettino, *Phys. Rev. Lett.* **88**, 85505 (2002).

Chromium Isotopes and the Fate of Hexavalent Chromium in the Environment

Andre S. Ellis,¹ Thomas M. Johnson,^{1*} Thomas D. Bullen²

Measurements of chromium (Cr) stable-isotope fractionation in laboratory experiments and natural waters show that lighter isotopes reacted preferentially during Cr(VI) reduction by magnetite and sediments. The $^{53}\text{Cr}/^{52}\text{Cr}$ ratio of the product was 3.4 ± 0.1 per mil less than that of the reactant. $^{53}\text{Cr}/^{52}\text{Cr}$ shifts in water samples indicate the extent of reduction, a critical process that renders toxic Cr(VI) in the environment immobile and less toxic.

Chromium is a common contaminant in surface water and groundwater (1, 2) because it is used widely in electroplating and other

industries and occurs naturally at high concentration in ultramafic rocks. Under oxidizing conditions, Cr is highly soluble and mobile as the Cr(VI) anions chromate (CrO_4^{2-}) and bichromate (HCrO_4^-). Cr(VI) is a suspected carcinogen (3). Under reducing conditions, Cr(VI) may convert to Cr(III), which is insoluble, strongly adsorbed onto solid surfaces (4), and less toxic. Cr(VI) can be removed from solution artificially by in situ reduction (5, 6), or naturally by reductants

¹Department of Geology, University of Illinois at Urbana-Champaign, 245 Natural History Building, Urbana, IL 61801, USA. ²Water Resources Division, U.S. Geological Survey, 345 Middlefield Road, Menlo Park, CA 94025, USA.

*To whom correspondence should be addressed. E-mail: tmjohnsn@uiuc.edu



**Geochemistry
Geophysics
Geosystems**

G³

AN ELECTRONIC JOURNAL OF THE EARTH SCIENCES

Published by AGU and the Geochemical Society

Technical Brief

Volume 2

July 3, 2001

Paper number 2000GC000124

ISSN: 1525-2027

Determination of molybdenum isotope fractionation by double-spike multicollector inductively coupled plasma mass spectrometry

Christopher Siebert, Thomas F. Nägler, and Jan D. Kramers

Isotopengeologie, Mineralogisch-Petrographisches Institut, Universität Bern, CH-3012 Bern, Erlachstrasse 9a, Switzerland (siebert@mpi.unibe.ch; naegler@mpi.unibe.ch; kramers@mpi.unibe.ch)

Natural mass-dependent variations in the isotopic composition of molybdenum

J. Barling^{a,*}, G.L. Arnold^a, A.D. Anbar^{a,b}

^a *Department of Earth and Environmental Sciences, University of Rochester, Rochester, NY 14627, USA*

^b *Department of Chemistry, University of Rochester, Rochester, NY 14627, USA*

Received 17 May 2001; received in revised form 7 September 2001; accepted 13 September 2001

Anal. Chem. **2001**, 73, 1425–1431

Precise Determination of Mass-Dependent Variations in the Isotopic Composition of Molybdenum Using MC-ICPMS

A. D. Anbar^{*,†,‡}, K. A. Knab[‡] and J. Barling[†]

Department of Earth and Environmental Sciences and Department of Chemistry, University of Rochester, Rochester, New York 14627

展望... ..

分析方法发面：

整体样品分析（**bulk sample analysis**）

→ 原位微区分析

整体而言：

方法研发 → 同位素示踪理论

整体而言：

探索性研究→ 聚焦重大科学问题

地球科学应用：

太阳系与行星早期演化

地球科学应用：

地球环境氧化还原状态演化

地球科学应用：

生命营养元素循环与生物环境协同演化

地球科学应用：

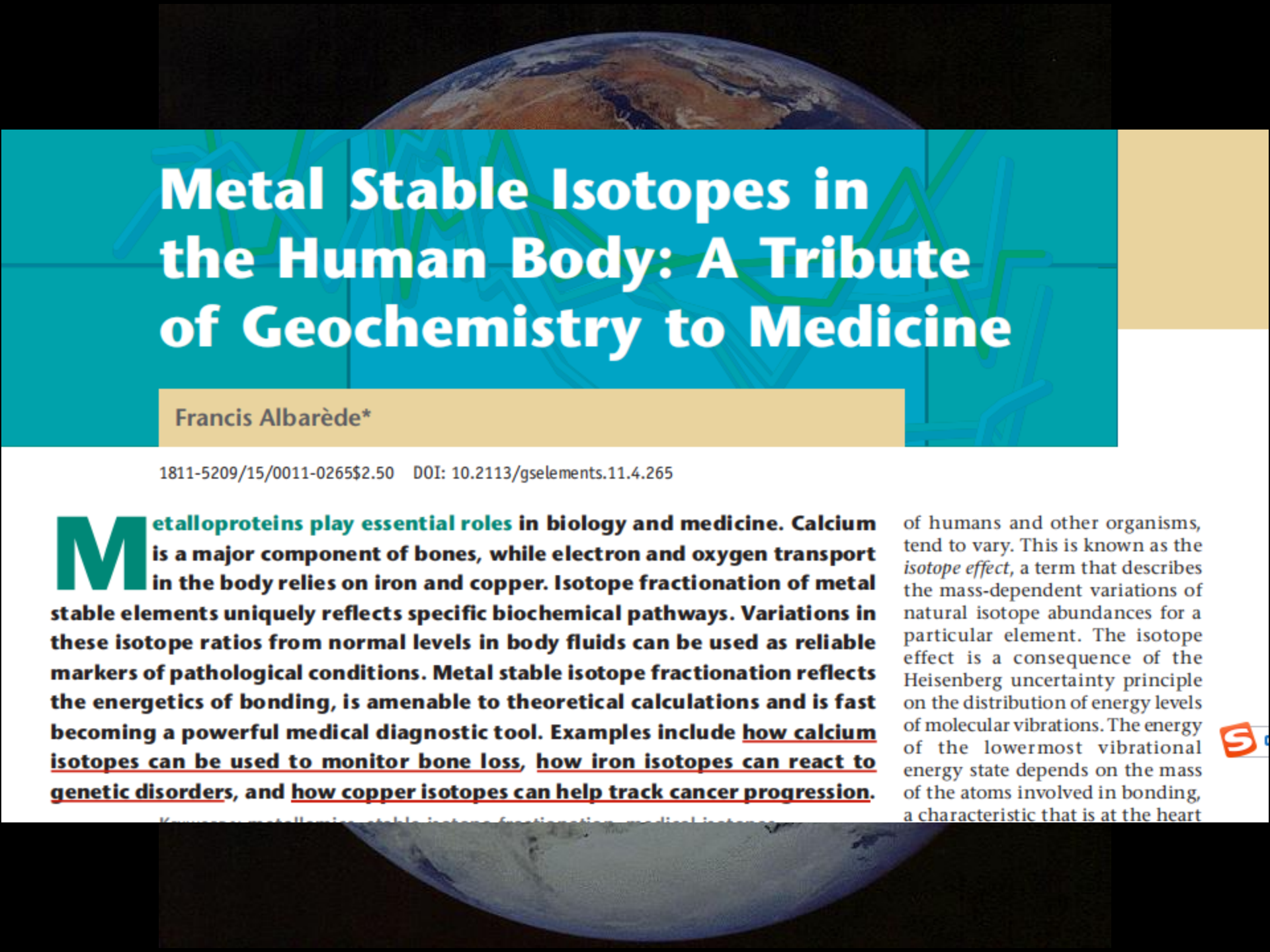
生命营养元素循环与生物环境协同演化

地球科学应用：

成矿作用与找矿勘探

地球科学应用：

环境科学：重金属污染评估与溯源



Metal Stable Isotopes in the Human Body: A Tribute of Geochemistry to Medicine

Francis Albarède*

1811-5209/15/0011-0265\$2.50 DOI: 10.2113/gselements.11.4.265

Metalloproteins play essential roles in biology and medicine. Calcium is a major component of bones, while electron and oxygen transport in the body relies on iron and copper. Isotope fractionation of metal stable elements uniquely reflects specific biochemical pathways. Variations in these isotope ratios from normal levels in body fluids can be used as reliable markers of pathological conditions. Metal stable isotope fractionation reflects the energetics of bonding, is amenable to theoretical calculations and is fast becoming a powerful medical diagnostic tool. Examples include how calcium isotopes can be used to monitor bone loss, how iron isotopes can react to genetic disorders, and how copper isotopes can help track cancer progression.

of humans and other organisms, tend to vary. This is known as the *isotope effect*, a term that describes the mass-dependent variations of natural isotope abundances for a particular element. The isotope effect is a consequence of the Heisenberg uncertainty principle on the distribution of energy levels of molecular vibrations. The energy of the lowermost vibrational energy state depends on the mass of the atoms involved in bonding, a characteristic that is at the heart





ORIGINAL PAPER

Potential of non-traditional isotope studies for bioarchaeology

Klervia Jaouen¹ · Marie-Laure Pons²

Received: 31 March 2016 / Accepted: 20 October 2016 / Published online: 3 November 2016

© The Author(s) 2016. This article is published with open access at Springerlink.com

Abstract As a consequence of recent developments in mass spectrometry, the application of non-traditional stable isotope systems (e.g. Ca, Cu, Fe, Mg, Sr, Zn) as well as radiogenic isotopes to archaeological materials is now possible. These techniques have opened new perspectives in bioarchaeology and can provide information on metabolism, diet and the mobility of past individuals. This review demonstrates this potential and describes the principle of these new analytical approaches. In addition, we emphasize how the “non-traditional” stable isotope systems compare and contrast with classic isotopic analyses.

Keywords Archaeological sciences · Metal stable isotopes · Tracers · Diet · Mobility · Metabolism

time, as opposed to radioactive isotopes that decay into a daughter isotope from a different element. This resulting daughter element is radiogenic. Radiogenic isotope abundances are typically expressed as the ratio of the radiogenic isotope of interest to a stable isotope of the same element (e.g. $^{87}\text{Sr}/^{86}\text{Sr}$). For stable isotope systems, the isotopic abundance is mostly measured in terms of delta notation (e.g. $\delta^{18}\text{O}$). If a radiogenic isotope is involved, then the results are usually expressed as isotopic ratios.

For several decades, radiogenic isotopes strontium (Sr) and lead (Pb) and stable isotopes of light elements (hydrogen (H), carbon (C), nitrogen (N), oxygen (O), sulphur (S)) were the main isotopic systems studied in human remains (Fig. 1). Detection of natural stable isotope abundances for elements of masses greater than 40 amu was very difficult until recently. Two decades ago, the development of multi-collector induc-



谢谢大家!